# Crashworthiness Research of Prototype Hydrogen Fuel Cell Vehicles:
# Task Order 7 Project Report

DISCLAIMER

This publication is distributed by the U.S. Department of Transportation, National Highway Traffic Safety Administration, in the interest of information exchange. The opinions, findings, and conclusions expressed in this publication are those of the authors and not necessarily those of the Department of Transportation or the National Highway Traffic Safety Administration. The United States Government assumes no liability for its contents or use thereof. If trade or manufacturers' names or products are mentioned, it is because they are considered essential to the object of the publication and should not be construed as an endorsement. The United States Government does not endorse products or manufacturers.

Suggested APA Format Citation:

Batelle Memorial Institute. (2015, February). *Crashworthiness research of prototype hydrogen fuel cell vehicles: Task order 7 project report.* (Report No. DOT HS 812 112). Washington, DC: National Highway Traffic Safety Administration.

# TABLE OF CONTENTS

<u>LIST OF APPENDICES</u>

<u>LIST OF TABLES</u>

# EXECUTIVE SUMMARY

Two prototype fuel cell vehicles that had been retired from a vehicle demonstration program were made available to the National Highway Traffic Safety Administration for research crash tests. The purpose of the tests was to evaluate test procedures to assess the safety performance of the high-pressure hydrogen fuel storage containers and the electrical isolation of high-voltage powertrain components in the crash test environment. One vehicle was crashed on the rear, essentially following NHTSA's test procedure for Federal Motor Vehicle Safety Standard (FMVSS) No. 303; Fuel system interity of natural gas vehicles. The other was crashed on the side, modeling FMVSS No. 301; Fuel system integrity, which applies to vehicles using liquid fuels. These crash conditions provide understanding of possible consequences of a controlled crash on a hydrogen fuel system and a high-voltage electrical system. They resolved some key questions for specifying possible modifications to the test conditions and assessment criteria in the FMVSS to address the safety challenges that are unique to hydrogen fuel cell vehicles.

Current crash test procedures to assess fuel system integrity use surrogates for liquid fuels and natural gas to monitor fuel system leaks while minimizing the potential for a fuel-fed fire following the crash, shoud a leak occur. Pass/fail criteria are based on the quantity and leak rate of the fuel surrogate. FMVSS No. 301 specifies the use of Stoddard solvent as a substitute for liquid fuels and FMVSS No. 303 specifies the use of nitrogen as a substitute for compressed natural gas (CNG). SAE J2578 [27] allows for the use of helium or hydrogen to monitor fuel system leaks in hydrogen vehicle crash tests. When using helium as a substitute fill gas, the fuel cell stack is inactive as a high-voltage source. Special test procedures have been developed to assess the post-crashelectrical isolation of the inactive high-voltage sources from the vehicle chassis [3], and were applied in these tests.

In these tests, both of the fuel systems and the electrical isolation systems survived the crashes: surrogate fuel did not leak and the electrical isolation was intact following the crashes. The fuel system was deformed by the impact, particularly in the rear crash, but remained intact.

This work was a follow-on to a set of three developmental crashes conducted in the fall of 2010 [5]. The small sedans in those crashes were production CNG vehicles that had been modified to have a mockup hydrogen fuel system. Each vehicle in the prior crash tests had a single fuel container in the trunk and was tested with hydrogen as the fill gas. Test procedures were developed to monitor hydrogen leakage and to provide capability to remotely defuel the vehicles after the test so that laboratory personnel did not approach vehicles with high-pressure gas stored in onboard containers that might have been compromised in the test. No electrical system evaluation was conducted on the vehicles because they did not contain fuel cell stacks or propulsion batteries.

The sport utility vehicles (SUVs) in the present project each had an 80-kW fuel cell stack under the hood, a set of three fuel containers mounted transversely under the body, and an auxiliary lithium-ion propulsion battery under the rear cargo area. These vehicles were prototypes that had been retired from service. The fuel cell stacks were deemed to be inoperable because they were aged beyond their useful life. Therefore, these vehicles were useful for assessing fuel container integrity with helium as the substitute fill gas, and electrical integrity with inactive high-voltage sources. In order to restrict the assessment of test procedures to those that monitor leakage,

container integrity, and isolation of inactive high-voltage sources, modifications to the vehicles were made as follows.

The lithium ion propulsion batteries were removed from the vehicles to minimize the risk of battery fire. However tests were conducted to assess the post-crash isolation of the battery housing from the vehicle chassis.

Only the container closest to the impact point in each crash was pressurized and monitored for leakage after the crash. This was done to simplify fill and venting procedures. If a failure were to occur, it would most likely be to the container in the location most vulnerable to impact. The other two containers were unpressurized and open to the atmosphere.

The rearmost container in the rear impacted vehicle was filled to 10 percent of service pressure (35 bar). This was determined to be the worst case fill pressure for laterally mounted containers being struck on the side because the container is less stiff at 10 percent fill and suffers more deformation [5].

The front most container in the side impacted vehicle was filled to 100 percent of service pressure (350 bar), because previous tests indicated that extreme impacts on the dome end may be more damaging to fully pressurized containers than to partially pressurized containers.

## Crash Results

Pre-crash photographs of the two vehicles are in Figure ES-1 and Figure ES-2. The fuel storage system was a set of three containers, as shown in Figure ES-3. Two containers were mounted in front of the rear wheels, and one was mounted between the rear wheels and bumper.

The rear-impact crash, with the billboard barrier according to FMVSS No. 303, pushed the rear bumper into the rear container, collapsing the components of the fuel system together. Containers showed surface damage, but the pressure boundary remained intact. The fuel system for the rear impact had been pressurized with helium to 35 bar (508 psi). This pressure, 10 percent of the container's service pressure, was selected to allow greater circumferential deformation, and greater potential for container damage. The structure of the vehicle protected the fuel system from the side-impact crash (conducted with the moving deformable barrier according to FMVSS No. 214). The fuel system was shaken during the impact, but suffered no observable or measurable damage. The fuel system for the side crash had been pressurized to 350 bar (5,076 psi) with a mixture of 80 percent helium and 20 percent nitrogen. One hundred percent of the service pressure was selected for the crash directed at the end of the container because full pressure proved to be the worst case in longitudinal impacts under extreme conditions in Task Order 1. A mixture of nitrogen and helium was used because it met the experimental requirements for leak detection and was significantly less expensive than pure helium. A helium sensor, provided by the National Renewable Energy Laboratory, which was mounted near the container, detected a trace amount of helium at the moment of impact. The sensor in the passenger compartment detected no helium. After the crash, both detectors were tested, and both detectors were found to be working correctly.

Electrical isolation between high-voltage components and the chassis was measured at several test points before and after both crashes. The crashes did not measurably change the isolation at any of the test points.



Figure ES-1. The rear crash was patterned after FMVSS No. 303, a "billboard" barrier at nominal 30 mph. The nets for containing debris in the event of a container rupture are visible behind the vehicle. The fuel system was pressurized to 35 bar (508psi) with helium.
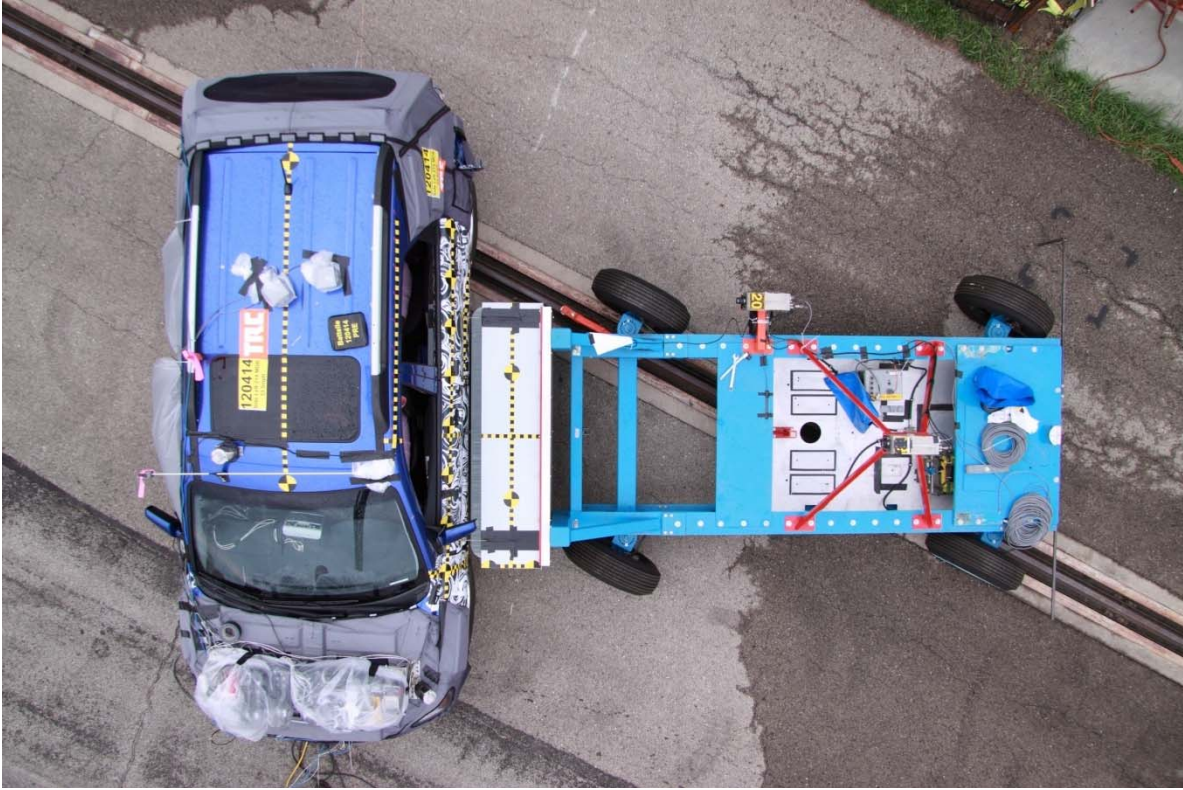
Figure ES-2. The side crash was patterned after FMVSS No. 301, which is identical to the dynamic impact in FMVSS No. 214. The moving deformable barrier's longitudinal axis is at an angle of 27 degrees to its direction of travel at nominally 33.5 mph. The fuel system was pressurized to 350 bar (5,076psi) with 80 percent helium and 20 percent nitrogen.
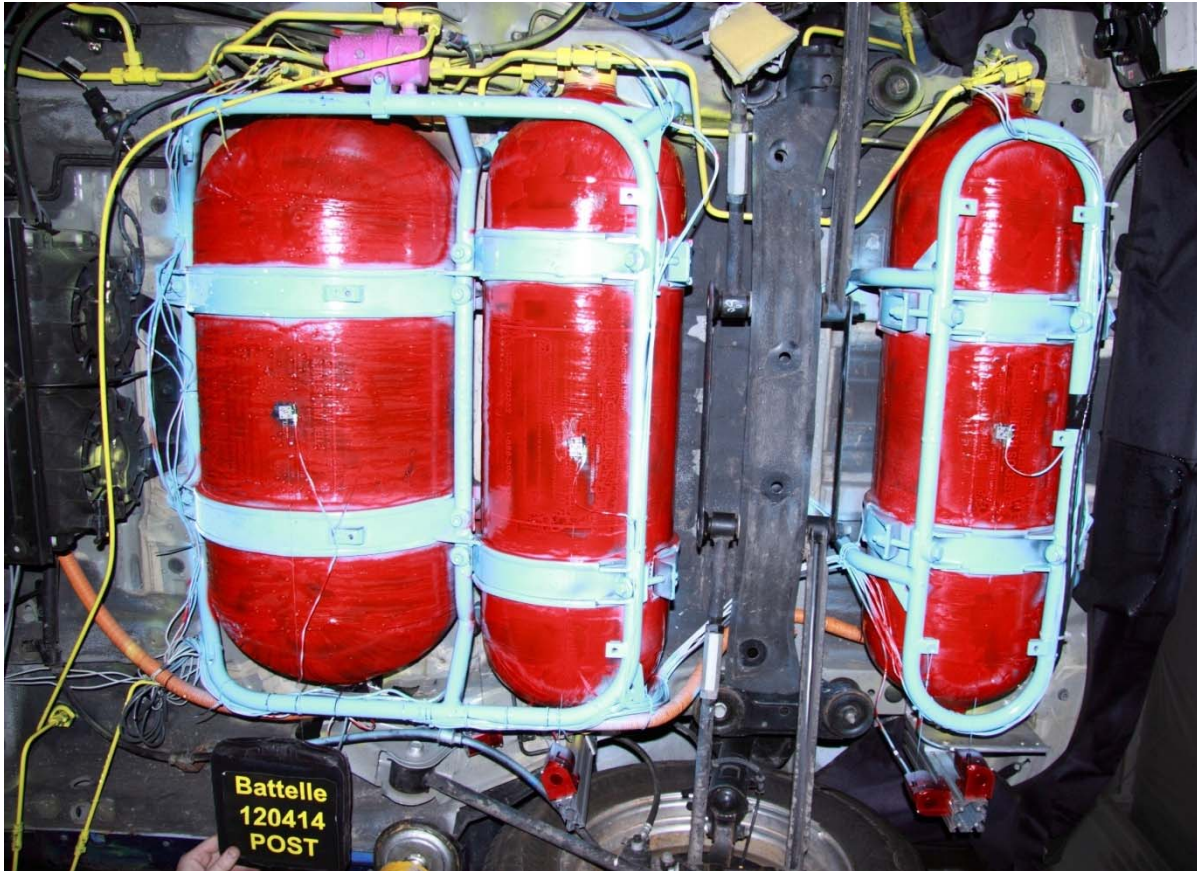
Figure ES-3. The vehicles had three fuel containers (painted red) mounted in straps (painted blue). The high-pressure stainless steel lines are painted yellow. The low-pressure regulator at the top of the photo is painted purple. The front of the vehicle is to the left.

# Implications

All five crashes in the two task orders showed that these particular fuel systems sustained damage but did not release hydrogen.

To protect test personnel from any sudden release from the containers, Battelle developed a system for safely and remotely releasing the containers' contents following the crash. The system requires modifications to the manufacturer's fuel system and would not be appropriate for a compliance test.

All the options for filling the fuel system for a compliance test have advantages and disadvantages. The seemingly natural choice, helium, is disadvantageous because it is much more expensive than the other gases and its availability is limited. Hydrogen, if it leaks, can be detected in small quantities, but crash testing with hydrogen requires extra care and safety precautions. If the container were pressurized with nitrogen, it would be impossible to detect leaks as small as necessary, either with pressure transducers or gas sensors. A possible compromise is a mixture of mostly nitrogen with a small amount of hydrogen or helium. Such standard mixtures are available from industrial gas suppliers for leak testing.

Electrical isolation measurements at the fuel cell are sensitive to the condition of the coolant. Coolant fluid that is aged or at high temperature as it could be in service will have a lower isolation; cooler and freshly flushed coolant provides for a pristine, higher isolation. Consequently, specifying the condition of the coolant is important to a meaningful isolation mesurement.

Certain plausible forms of damage to the electrical isolation will evade detection by conventional test points. Means of measuring isolation on the high-voltage side of automatic cutoffs can detect this kind of damage.

# Related Task Orders

Hydrogen fueled motor vehicles offer many advantages in terms of pollution and efficiency over gasoline-fueled vehicles. At the same time, they pose hazards that are not necessarily more severe, but are certainly different from those in vehicles with gasoline fuel. NHTSA has contracted a team, led by Battelle, to generate technical data for NHTSA to consider in writing safety rules for hydrogen fuel vehicles.

NHTSA's hydrogen research program includes six previous task orders, which are listed below. The present project, Task Order 7, extended the work of Task Orders 1, 4, and 6.

- Compressed Hydrogen Container Fuel Options for Crash Testing (Task Order 1) [5]. This task order included leak rate characterization, dynamic impact crush tests on containers, and crash tests of three vehicles with mockup hydrogen fuel systems. The two crash tests in the present report are a direct follow-on to this task order.

- Durability Testing (Task Order 2) [15]. The integrity of containers was assessed after they experienced pressurization and temperature cycles intended to simulate a lifetime of harsh service.

- Post-Crash Hydrogen Leakage Limits and Fire Safety (Task Order 3) [4]. This task order provided data to support assessments of acceptable post-crash leakage rates. Hydrogen gas was leaked at controlled rates into a passenger car interior, and the rate, location, and ultimate concentration were measured. A spark was then used to ignite any accumulated hydrogen, and the consequences to the vehicle and to crash dummies, simulating occupants, were measured. The experiment was repeated for a number of different leak rates.

- Electrical Isolation (Task Order 4) [3]. Battelle developed and verified an alternative electrical isolation test procedure for hydrogen fuel cell vehicles. The refined final procedure was performed on two hydrogen fueled vehicles, confirming that the detailed steps and instrumentation can accurately test electrical isolation on an inactive fuel cell.

- Published Literature Review (Task Order 5). The final report on this project [2] cited more than one hundred references on hydrogen dispersion and ignition, tests of the container, fast fueling, and incidents. Findings were discussed in light of NHTSA's needs.

- Electrical Protective Barrier (Task Order 6). Battelle assessed electrical protective barriers as a means of providing electrical safety following a crash. Analysis and testing demonstrated that electrical isolation must be used concurrently with conductive barriers to ensure safety.

# 1.0  INTRODUCTION

To ensure fuel system integrity of passenger vehicles in crashes, NHTSA has promulgated regulations that impose limits on post-crash fuel leakage under representative crash conditions. These conditions are defined in FMVSS Nos. 301, Fuel System Integrity [9], and 303, Fuel System Integrity of Compressed Natural Gas Vehicles [11]. FMVSS No. 301 limits liquid fuel leakage to one ounce per minute for 30 minutes post crash, and FMVSS No. 303 limits the leakage of natural gas to an energy equivalent measured by a post-crash pressure drop in the high-pressure portion of the fuel system. Similar testing requirements may need to be developed for hydrogen-fueled vehicles.

Toward this end, NHTSA has tasked a team led by Battelle to evaluate various technical aspects of the safety of hydrogen fueled vehicles. Battelle was the prime contractor leading a team to conduct these experiments. Battelle led the team that recently completed a series of crashes on vehicles with mockup hydrogen fuel systems [5]. The two vehicles crashed in the present project were non-working hydrogen fuel cell prototypes that had been retired from a demonstration program.

Battelle was responsible for the overall organization of the present project and analysis of the data. The Transportation Research Center, Inc., conducted the crashes and advised NHTSA and Battelle on crash test procedures.

## 1.1  Differences in Hydrogen Storage

Liquid fuels such as gasoline are stored on vehicles at essentially atmospheric pressure. Gaseous fuels, such as hydrogen and natural gas, need to be compressed to high pressures to store a reasonable amount of energy within the volume available on the vehicle. To hold these high pressures, compressed gas fuel containers need to be mechanically stronger than the crashworthy liquid fuel containers. Hydrogen is also present in tubing outside the container, along with fittings such as elbows and tees. Although severe damage to the external tubing can lead to a leak, valves in the container limit the amount that can leak. In the vehicles tested, a solenoid is de-energized and closes when the airbag sensors trigger. An excess flow valve was present to limit the flow rate should external tubing be sheared when the valve is still open.

Containers for pressurized gas fuel in motor vehicles are constructed differently than containers for liquid gasoline, so they are susceptible to different kinds of damage. Containers for hydrogen are built differently than those for compressed natural gas, so they, too, must be tested separately.

The purpose of the crash tests was to document the behavior of representative fuel systems in established crash test conditions, with the goal of developing crash tests suitable for hydrogen fuel systems.

## 1.2    Electrical Isolation Measurements

The possibility of a fire resulting from a fuel container leak is only one hazard of a hydrogen fuel cell crash. Whereas the electrical system in a conventional gasoline vehicle is predominantly 12 V, the fuel cell and the associated inverter and electrical motors will have potentials of several hundred volts. Furthermore, the combination of AC and DC voltages may pose a more complicated hazard to people should the electrical system become compromised in a crash.

The purpose of performing isolation measurements on prototype fuel cell vehicles was twofold: to assess the degree of electrical safety, and to evaluate how measurements could be performed and interpreted in eventual compliance tests for fuel cell vehicles with similar electrical architectures.

# 2.0 TEST PROCEDURE

The team crashed two hydrogen fuel cell SUVs adhering closely to the conditions of FMVSS No. 303 and FMVSS No. 301. The crashes were recorded by video cameras and accelerometers as is usual for these crashes, with additional accelerometers and string potentiometers to document the fuel system motion. The vehicles carried helium sensors to document the survivability of the sensors and to detect any helium following the crashes. The electrical isolation between the high-voltage system and the vehicle chassis were measured before and after the crashes.

The complete test plan is in Appendix A. The electrical isolation measurement procedure is in Appendix B.

## 2.1 Crash Conditions

The crashes followed as much as possible the conditions of the rear crash in FMVSS No. 303 and the side crash of FMVSS No. 301, and NHTSA's associated test procedures [16] [18]. Because these were research experiments and not compliance tests, there were minor departures from the formal test procedures. Schematics of the crash conditions from NHTSA's test procedures are in Table 2-1. Table 2-2 lists the nominal test conditions.
Both vehicles had ballast dummies. The camera layout was according to the NHTSA test procedure for the rear crash; not all of the standard cameras were used for the side crash, and one camera was mounted on the rear bumper to observe the containers' valve ends.

The side crash target impact point for the moving deformable barrier was according to the NHTSA test procedure. The face of the honeycomb barrier encompassed the width of the forward fuel container. The two other containers were aft of the impact zone. This is contrasted with the 2010 passenger car crashes where the moving deformable barrier had been aimed aft of the standard FMVSS location, to strike the entire high-pressure fuel system.

In this, Task Order 7, two OEM prototype SUVs were tested. These fuel systems consisted of three Type 3 containers, one 74 L and two 39 L, which were strapped into two steel tube mounting frames. Specifications of the containers are in Table 2-3. These frames were bolted to the underside of the vehicle. In the OEM design, two sheet metal covers were secured to container mounting frame to help protect the containers. One covered the front and middle containers, while the second covered only the rear container. These sheet metal covers provided minimal structural rigidity to the vehicle and were predominantly used to shield the containers from road debris. To improve visibility of the containers during testing, these metal covers were removed.

The stainless steel tubing used in the SUVs was 10 mm outer diameter with a wall thickness of 2 mm. This tubing is rated for a working pressure of approximately 448 bar (6,500 psi). In addition the stainless steel fittings and tees were rated for a dynamic working pressure of 414 bar (6,000 psi). The tubing was flanged to 90 degrees and seated against a captive O-ring seal in each fitting. The containers were Type 3, carbon fiber wrapped aluminum shell, and were rated for a service pressure of 350 bar (5,076 psi). The solenoid end valves were GFI Teleflex XTV-110 and rated for 350 bar (5,076 psi) [29].

Only one container—the one in the most vulnerable location—was pressurized in each crash. The rear container was pressurized for the rear crash, and the forward container was pressurized for the side crash. The two unpressurized containers were open to atmosphere. This was done to minimize the consequences of a pressurized gas release, in the unlikely event of a fuel system failure.

The reports from TRC Inc. in Appendix D and Appendix E document the full set of actual crash conditions, camera locations, and high-speed data.

Table 2-1. Schematics of the test conditions and camera locations.

| | Test Procedure | Graphic |
|---|---|---|
| Rear | TP-303-00 [17] (References TP301-4) [16] |  |
| Side | TP301-04 [16] (References TP-214D-08 [18] |  |
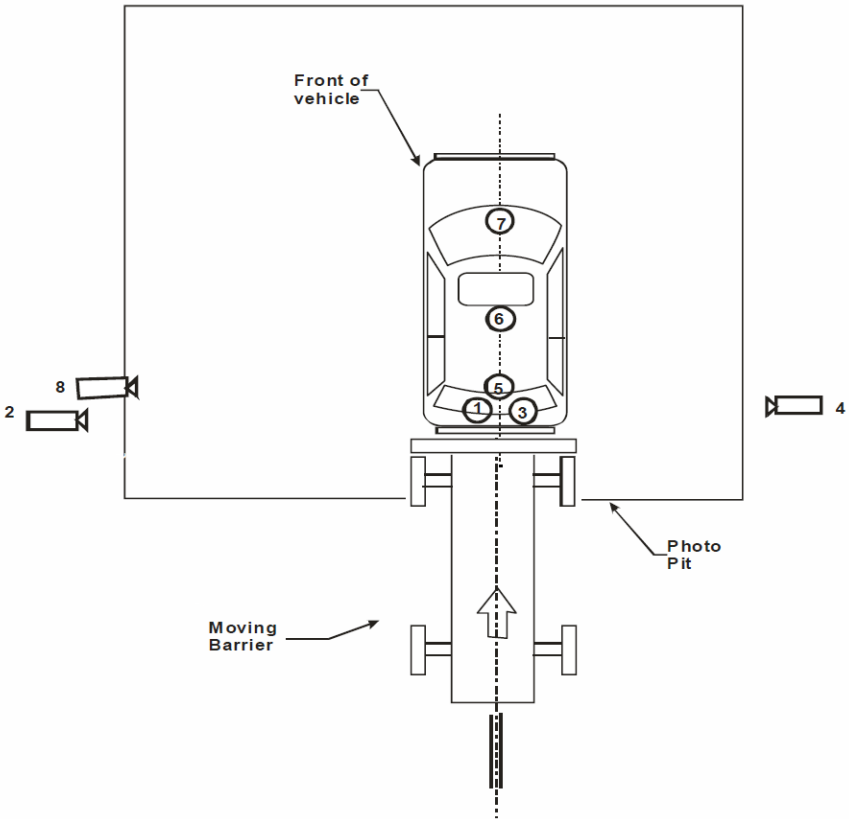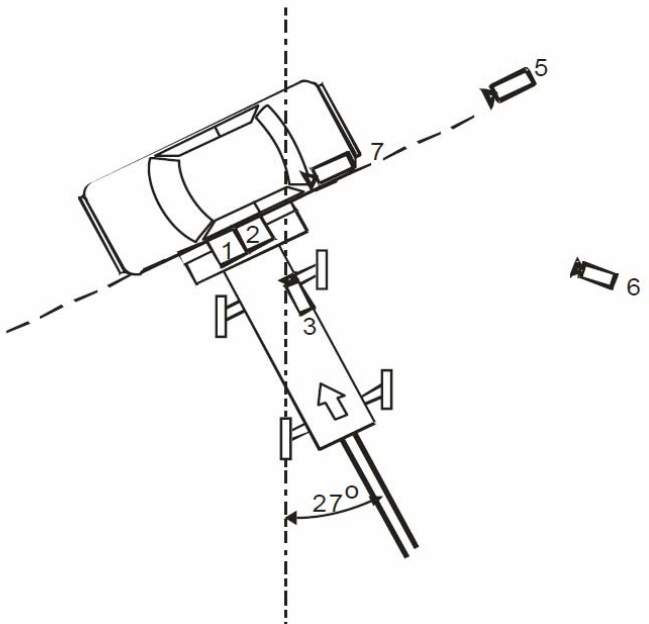
Table 2-2. Nominal conditions of these crashes, compared with the NHTSA test procedures.

| | | FMVSS 303 (S6.2) | FMVSS 301 (S6.3b) FMVSS 214 (S8) | Planned Crash |
|---|---|---|---|---|
| Test Procedure | | TP-303-00 [11] | TP-214D-08 [17] | (Appendix A of this document) |
| Rear | Speed | (48 kph) 30 mph | | (48 kph) 30 mph Actual speed: 48.0 kph |
| | Barrier | billboard | | billboard |
| | Alignment | centerline on centerline | | centerline on centerline |
| | Fill | 96 to 98% of service pressure Nitrogen | | 35 bar (500 psi) (10% of service pressure) Helium in the rear container |
| Side | Speed | | 53 kph (33.5 mph) | 53 kph (33.5 mph) Actual speed: 53.1 kph |
| | Barrier | | moving deformable | moving deformable |
| | Approach | | 27° crab angle | 27° crab angle |
| | Fill | | Stoddard solvent | 350 bar (5000 psi) (100% of service pressure) 80% Helium and 20% Nitrogen in the forward container |
| Ballast | | two front seat dummies | dummies in the front and rear outboard seats on the struck side | two ballast dummies: front seat (rear crash) struck side (side crash) |
| Post-crash Rotation | | No | Yes | No |
| Post-crash Wait | | 1 hour | 30 minutes | 1 hour |
| Permissible Leak | | Greater of 1062 kPa drop OR 895 $(T/V_{FS})$ kPa | 28 g/min | This was not a compliance test so there was no failure criterion. |

Table 2-3. Hydrogen fuel containers in the prior and current crashes.

| | Task Order 01 [5] | Current Crashes | |
|---|---|---|---|
| | | Forward Container | Middle and Rear Containers |
| Construction | Type 4 | Type 3 | Type 3 |
| Manufacturer | Lincoln Composites | Dynetek | Dynetek |
| Service Pressure | 350 bar | 350 bar | 350 bar |
| Water Volume | 65 L | 74 L | 39 L |
| Mass | 32 kg | 36 kg | 20 kg |
| Diameter | 400 mm | 399 mm | 280 mm |
| Length | 815 mm | 900 mm | 926 mm |
| Nominal Capacity | 1.57 kg $H_2$ | 1.79 kg $H_2$ | 0.94 kg $H_2$ |

These crashes extended the work of the three 2010 research crashes. Like the 2010 crashes, these crashes were patterned after NHTSA's compliance test procedures. There were many similarities between the two task orders, and there were significant differences in the vehicles and the test procedures. Table 2-4 summarizes the major differences between the two sets of crash tests.

Table 2-4. Conditions of the current and previous test crashes.

| | Task Order 01 [5] | Current Crashes |
|---|---|---|
| Base Vehicle | Small Sedan | SUV |
| Fuel System | CNG, converted to a mockup hydrogen system | hydrogen fuel cell |
| Container Location | in the trunk | under the body |
| Date of Crashes | September and October 2010 | April 2012 |
| Crash Conditions | FMVSS 301 [9] front, side, and rear | FMVSS 303 [11] rear FMVSS 301 [9] side (See Table 2-1) |
| Side crash target | aft of the standard, spanning the rear door to the fuel fill cap | according to the NHTSA test procedure |
| Container Construction (See Table 2-3) | Type 4 | Type 3 |
| Number and Water Volume of the Containers (See Table 2-3) | One 65 L | One 74 L Two 39 L |
| Container Fill (See Table 2-2) | Hydrogen | Helium in the 39-L rear container (rear crash) 80% Helium 20% Nitrogen mixture in the 74-L front container (side crash) |

Figure 2-1 shows the impact zone in the side crash with respect to the locations of the three fuel containers.



Figure 2-1. The red-and-white targets are aligned with the three fuel containers. One target is on the sill below the rear door, and two are on the rear tire. The forward container was within the span struck by the moving deformable barrier.

## 2.2   Measurements

Many measurements were made before, during, and after the crashes. Movement of the fuel system was characterized, similar to a compliance crash test, and pressure and temperature of the fuel simulant were measured. Helium sensors monitored the area around the fuel system and inside the passenger compartment. Electrical isolation at key test points was measured manually before and after the crashes.

### 2.2.1  Crash Motion

An array of triaxial accelerometers was mounted on the body of each vehicle as in a compliance test. In addition, triaxial accelerometers were on both ends of all fuel containers so their motion was fully characterized. String potentiometers measured displacement between the two ends of each container and the vehicle body. The string potentiometers measured fore-aft motion in the rear crash and lateral motion in the side crash.

The acceleration response of the vehicle and fuel system was recorded using 36 Endevco 7264C piezoresistive accelerometers. These accelerometers were mounted in accordance with SAE J211 [25] and sampled at a rate of 10 kHz. The vehicle and fuel system accelerations were filtered in accordance with SAE J211, CFC-60.

Signals from these two kinds of sensors were compared with the high-speed video and with physical assessments of the damage after the crash.



Figure 2-2. A triaxial accelerometer is visible on the valve, which is on the driver side of the rear container. Similar triaxial accelerometers were mounted on both ends of all three containers on both vehicles. The string for the string potentiometer is attached to the hex stem on the solenoid end valve. String potentiometers measured longitudinal displacement in the rear crash (shown here) and lateral displacement in the side crash.

## 2.2.2 Pressure and Temperature

Pressure and temperature transducers monitored the gas in the one pressurized container before, during, and after the crash. The pressure measurements were essential for monitoring the fill and ensuring that the container was at test pressure immediately prior to the crash. AST4000 pressure transducers were used to monitor the internal container pressure as well as the regulated pressure, which leads to the fuel cell. The gas temperature inside the container was measured by means of the AD22100 temperature sensor that was part of the GFI Teleflex solenoid end

valve [29]. The discussion in Section 3.4.1 shows that the inherent measurement error in the transducers precludes detection of small leaks from only pressure and temperature measurements.

### 2.2.3 Helium Sensors

The Department of Energy's National Renewable Energy Laboratory (NREL) mounted crash-rated helium sensors on both vehicles [24]. These devices, which are sensitive to changes in the thermal conductivity of a gas, can detect the presence of helium or hydrogen. The primary purpose of their presence was to demonstrate that the sensors can survive the impact of the crash, but the output of two of them was monitored before, during, and after the side crash.

Five HLS-440P sensors were installed on each vehicle. For both the side and rear crash tests three of the sensors were located in the passenger compartment, mounted to the interior headliner directly above the passenger side rear seat. For the rear crash, two sensors were located in the rear driver side wheel well, as shown in Figure 2-3. In the side crash the exterior two sensors were located under the body about a foot forward of the front container's solenoid valve.



Figure 2-3. The two externally mounted helium sensors were in the driver side rear wheel well, above the two smaller fuel containers, as shown here for the rear crash. The electrical connector for a sensor is in the hand. A sensor was mounted under the vehicle near the valve of the forward container for the side crash.

## 2.2.4 Electrical Isolation

The electrical isolation measurements were obtained by following the test procedure written specifically for these crashes. The test procedure was based both on FMVSS No. 305 and a test procedure developed in prior work for NHTSA [3, Appendix A]. The test procedure is in Appendix B and the filled in log sheets are in Appendix C.

High-voltage sources were not energized in these tests. Section 6.3 of the Revised Draft global technical regulation on hydrogen and fuel cell vehicles [9] allows for testing isolation resistance with all or part of the electric powertrain deenergized. The test procedure was to apply a test voltage between each high-voltage source and the electrical chassis and measure the resulting leakage current. A multimeter was used to verify the absence of voltage at the test points before performing the isolation tests.

The chosen measurement instrument, a safety analyzer, is capable of performing multiple tests, including DC dielectric tests (DC Hipot, or high potential), AC dielectric tests (AC Hipot), insulation resistance (Megger test), and ground bond tests. The DC Hipot test is similar to the insulation resistance test, but displays leakage current instead of resistance, and allows quick charging of capacitive devices. The DC Hipot test was chosen as the method of determining electrical isolation to ensure that the test was performed with sufficient charging current, while avoiding the measurement errors associated with using a megohmmeter on grounded test devices. A conceptual diagram of the DC Hipot test is shown in Figure 2-4.
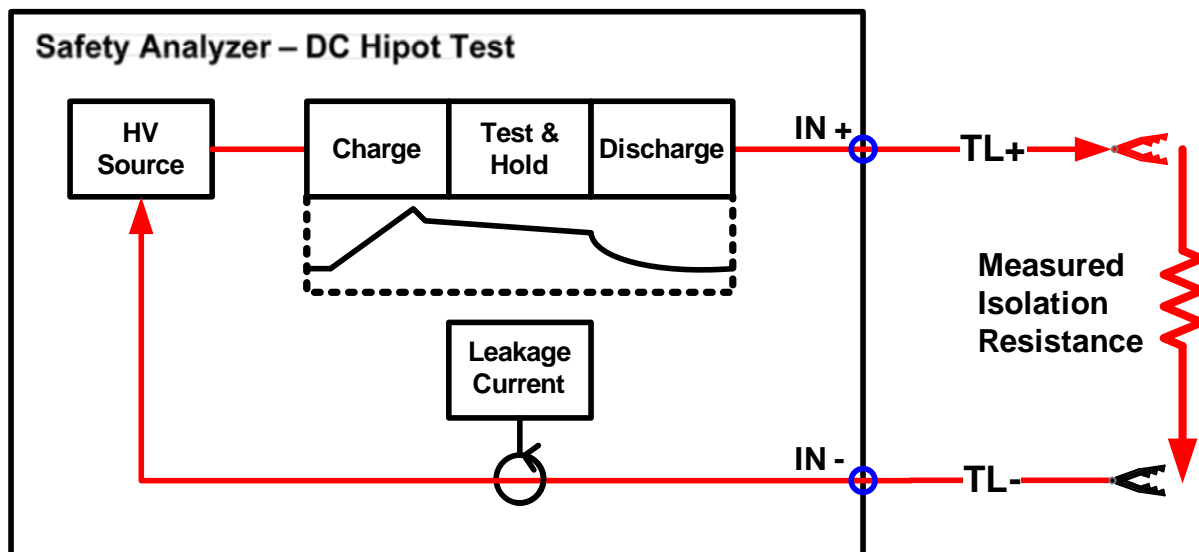


**Figure 2-4. Safety analyzer showing positive and negative test leads, TL+ and TL-**

Prior to electrical isolation measurements, the team identified a number of high-voltage sources normally present on a vehicle. The vehicles were inspected to identify accessible test points for each high-voltage source. These test points were electrically located as follows: at the ring terminals of the removed high-voltage battery, at the power train side of the fuel cell automatic disconnects, at the DC terminals of the motor control unit (MCU), and at the 3-phase AC terminals of the MCU.

Prior to performing electrical isolation tests, each of the high-voltage sources was rendered inactive, test points were prepared, and deionized water was added to each vehicle's fuel cell coolant reservoir. The high-voltage sources in these prototype crash tests were rendered inactive or removed, but this may not be necessary for eventual compliance tests. To render the high-voltage sources inactive, the high-voltage battery was removed, and the hydrogen for the fuel cell was replaced with helium, an inert substitute. For a future compliance test of a production vehicle following FMVSS No. 305 or a new revision, this step may not be necessary because the procedure is for active high-voltage sources. Each test point was prepared prior to testing so that a secure physical connection could be made between the safety analyzer test leads and the test points. The test points were located such that they were accessible at the time of the test without requiring excessive effort from the test operator.

One to three days before each pre-impact and post-impact test, deionized water was added to each vehicle's fuel cell coolant reservoir until water came through the open overflow tube on the underside of the vehicles. Allowing absorption to occur within the fuel cell membranes was desirable; however, the fuel cell coolant pump could not be started, and most of the coolant was aged water and absorption was not guaranteed.

Data was collected by applying a test voltage approximately 5 percent above the maximum nominal source voltage. The nominal battery voltage was 152 Vdc, so a test voltage of 160 Vdc was applied between the electrical chassis and each polarity of the high-voltage bus. The specified upper nominal fuel cell voltage was 460 Vdc, so a test voltage of 480 Vdc was applied. After examining the power converters on the underside of each vehicle, the assumption was made that the maximum MCU DC voltage was also 460 Vdc, so a test voltage of 480 Vdc was applied to the MCU DC lines. Finally, an assumption was made that the highest peak voltage on the 3-phase AC side of the MCU resulting from the DC to 3-phase AC inversion was 460 Vpeak, and a test voltage of 480 Vdc was again applied between each phase of the MCU AC lines and the electrical chassis.

Figure 2-5 shows a test operator ensuring no voltage was present at the test points before beginning a DC Hipot test. The next four figures show the safety analyzer connections for the fuel cell, MCU, and high-voltage battery lines. Figure 2-6 shows the safety analyzer connected to the fuel cell. Figure 2-7 is a close-up of how the safety analyzer positive test lead is electrically connected to the positive terminal of the fuel cell, while the negative test lead is electrically connected to the vehicle chassis. In Figure 2-8 the positive test lead of the safety analyzer is connected to one of the three phases of the MCU AC lines. Finally, in Figure 2-9, the positive test lead of the safety analyzer is connected to a ring terminal that is normally connected to the negative terminal of the high-voltage battery, while the negative test lead is connected to the vehicle's electrical chassis.

Figure 2-5. Test points were measured with a conventional multimeter to ensure that no voltage was present before the safety analyzer applied the high-voltage for the isolation tests.



Figure 2-6. The safety analyzer is attached to the fuel cell lines following the rear crash.
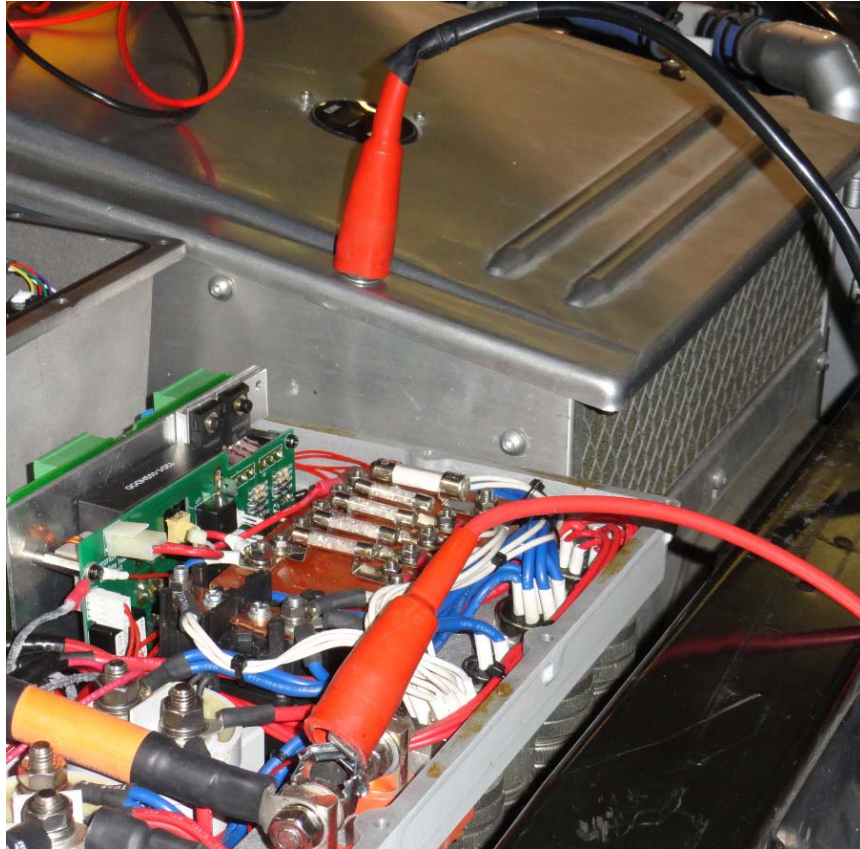
Figure 2-7. Close-up of the connections for testing the isolation of the fuel cell lines.
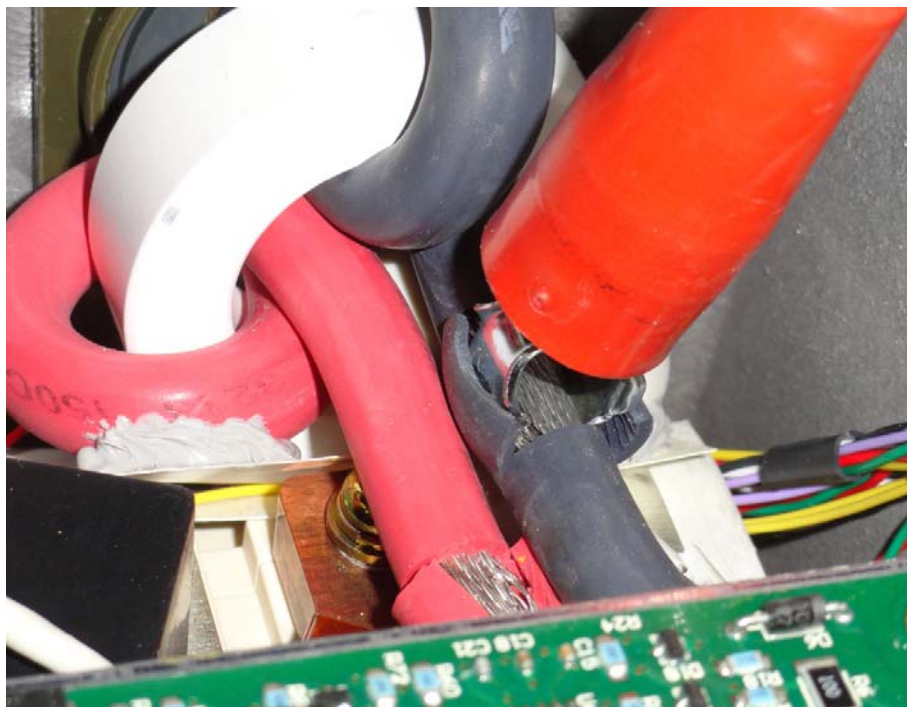


Figure 2-8. Close-up of the connections for testing the isolation of the MCU lines. Note where the insulation had been slit prior to the crash to simplify the attachments.

Figure 2-9. Close-up of the connections for testing the isolation of the line that runs to the high-voltage battery.

# 3.0 RESULTS

The crashes were conducted according to the test plan in Appendix A and the vehicles behaved as expected in FMVSS 301 and 303 compliance tests. Both fuel systems held their pressure during the hour-long hold following the crash, although the helium sensors detected trace amounts of helium seconds after impact and sporadically during the hour afterward. This section presents the results of the crashes and the analysis of the data.

## 3.1 Crash Conditions

The speeds, orientations, and impact points of both crashes were as intended. Exact conditions are in the reports of TRC, which are in Appendix D and Appendix E. The mass of the side crash vehicle was 23 kg above the intended 2,031 kg. The excess of less than two percent was judged to be unimportant for the research crash, so no further weight was removed.

A small portion of the data was unavailable due to equipment failures. In the rear crash, the helium sensor, pressure, and temperature data were not recorded during the post-crash hold. Backup indicators assured the team at the time that there was no gross loss of contents. The fuel system was pressurized again with helium following the crash and held pressure for one hour. Two string potentiometers malfunctioned during the side crash. Two video cameras of the side crash, the real time and one on the moving deformable barrier, did not trigger. The remaining data and videos were adequate to assess the conditions of the crashes and resulting damage.

## 3.2 Qualitative Description of Damage

When the billboard barrier struck the rear bumper, it pushed the bumper into the rear fuel container. The container and several components in front of it were pressed together in succession. The sequence is visible in the underbody videos, and it was confirmed by the surface marks evident when the fuel system was disassembled.

The fuel system during the side crash, moved momentarily, but contact between the containers and the vehicle body were minimal. As a result permanent deformation of tubing was minimal.

### 3.2.1 Qualitative Description of the Rear Crash

The billboard barrier pushed the rear bumper into the vehicle. The rear container moved forward within the vehicle, pushing a suspension cross member into the middle container. This sequence of events is visible in the high-speed video from the photo pit, and it is consistent with the recorded signals. The permanent deformation is visible in the pre- and post-crash photos in Figure 3-1. The string potentiometers show the rear container beginning to move with respect to the vehicle about 25 ms after impact, and the two forward containers begin to move 50 ms after impact. Most of the vehicle-mounted accelerometers recorded a peak forward acceleration on the order of 20 g, which is typical for a crash test. The rear container experienced a peak forward acceleration closer to 80 g, indicating it was struck more directly by the barrier through the bumper. The middle container's peak forward acceleration exceeded 120 g, which is consistent with the rear container's impact on the middle container, through the rear suspension bushings.
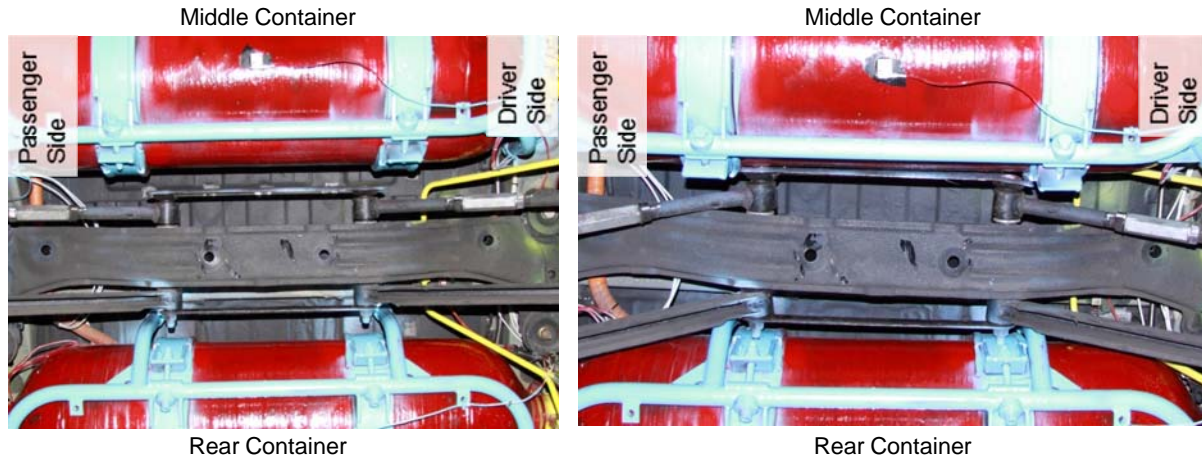
Figure 3-1. The gaps between the containers and the suspension are visible in the pre-crash photo on the left, which is looking up at the underside of the vehicle. The post-crash photo on the right shows that the gaps have closed. The straps for the rear container (painted blue) have been pushed forward into the suspension bolts, which in turn have moved into the side of the middle container. These are close-ups of Figures A-29 and A-30 in Appendix A.

The two steel straps that hold the rear container in its mounting frame were directly in line with two exposed bolt ends from the suspension. As the container was displaced forward in the rear crash, the steel straps contacted the bolts, leaving a mark in the paint on the passenger side strap (Figure 3-2). As a result of the bolts impacting the straps, the suspension cross member was pushed forward enough to contact the middle container. As was visible in Figure 3-1, the swing arm bolts align with the straps of the rear container, but were pushed directly into the middle container itself. Figure 3-3 shows the damage that the bolt caused to the wall of the middle container. Forward motion of the rear container caused forward displacement of the middle and front containers. Figure 3-4 shows a gouge of approximately 10 mm length where the front container was pushed into the underbody of the vehicle.

Figure 3-2. The suspension bolt caused this damage to the mounting strap for the rear container. The strap protected the surface of the container from abrasion and distributed the load of the bolt.

Figure 3-3. The impact drove the suspension bolt into the rear surface of the middle container. Two imprints of the bolt face are visible, indicating a rebound and second impact. Paint from the container was visible on the end of the bolt.

Figure 3-4. This gouge on the front surface of the forward container was caused by its contact with the underbody of the vehicle.

Some stainless steel tubing was permanently deformed as a result of the rear container's forward displacement during the crash. The most significant deformation was the on the pressure relief device (PRD) vent line exit. The PRD vent line protrudes out the rear of the vehicle and was contacted directly by the billboard barrier in the rear crash. The PRD vent line is not pressurized during normal operation and was not pressurized for this testing.

The mounting for the rear container was nearly torn away from its bolted attachment to the underbody.

Before and after the crash Faro Arm data was collected so that comparisons could be made between the original and deformed structures. In the rear crash it can be seen below that the rear bumper deflected a significant amount, while the rest of the vehicle remained relatively unchanged. Figure 3-5 and Figure 3-6 depict the vector displacement of the Faro Arm measurement locations on the vehicle body panels (blue) and the accelerometer locations (red).

Figure 3-5. Displacement vectors overlaid on a pre-test side view of the rear-crash vehicle.
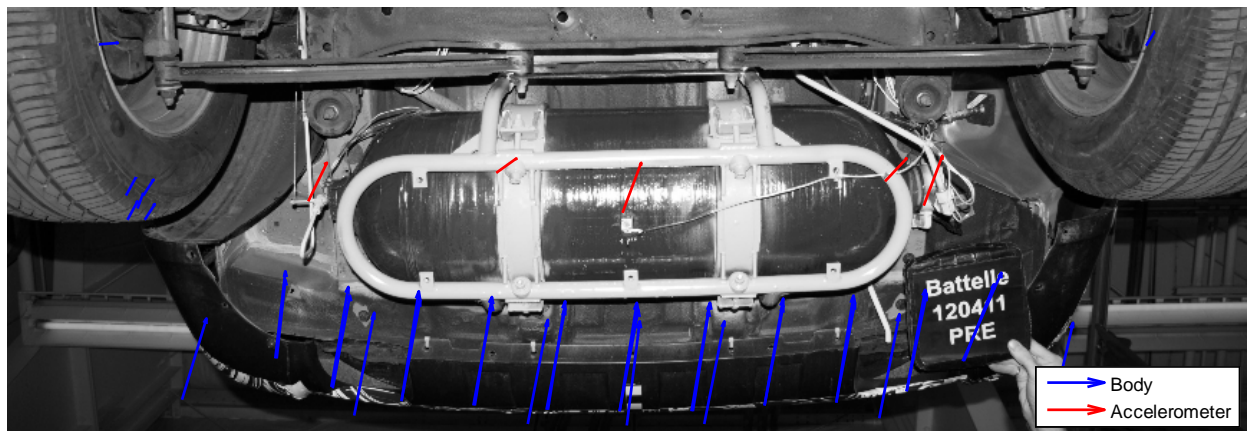


Figure 3-6. Displacement vectors overlaid on a pre-test bottom view of the rear-crash vehicle.

## 3.2.2 Qualitative Description of the Side Crash

The vehicle's structure offset the fuel containers and their valves from direct impact. The maximum accelerations recorded on the containers were all between 25 and 35 g, which are comparable to the maximum of the vehicle center of gravity. The string potentiometers and the onboard video camera both showed that the containers moved toward the struck side immediately after impact (more properly, their inertia held them still as the body moved toward

them), and then returned nearly to their initial location within the vehicle. When the fuel system was disassembled following the crash, clearance remained between the fuel components and the vehicle structure. Fuji Prescale pressure indicating film between the forward container solenoid valve and vehicle's underbody sidewall on the struck side showed no evidence of contact; the film on the opposite side showed light contact between a loose protective cap and the vehicle underbody. The light contact was attributed to handling and not a result of the crash. This cap was installed to protect a fitting installed by Battelle for direct access to the container as a part of the post crash vent system. In a production vehicle this cap would not be necessary and any contact between the cap and the vehicle underbody would likely not be an issue.

Similar to the rear crash, it can be seen from the vector data overlaid on the pre-test pictures that the vehicle used in the side crash deformed more where it was impacted by the moving barrier (Figure 3-7 and Figure 3-8). There was little overall deflection at any point. One important aspect to notice is the trend for arrows in the side view to be pointing downwards; this is likely due to the flat front driver side tire at the end of the test.
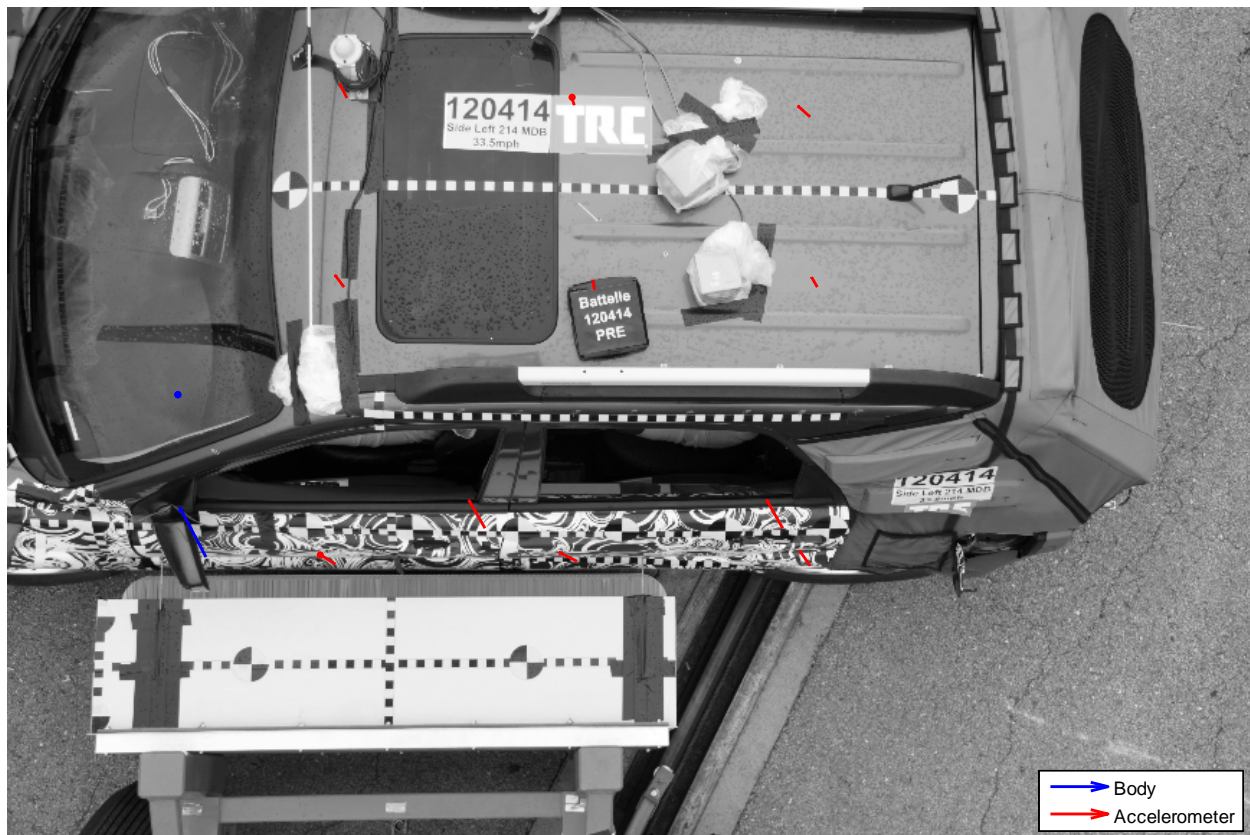


Figure 3-7. Displacement vectors overlaid on a pre-test top view of the side-crash vehicle.

Figure 3-8. Displacement vectors overlaid on a pre-test side view of the side-crash vehicle.

## 3.3    Transient Motion During the Crashes

### 3.3.1  Hydrogen Fuel System

One triaxial accelerometer was secured to each end of each of the three containers. An additional uniaxial accelerometer was mounted at the midpoint of each container to capture any pitch of the containers.

### 3.3.1.1  Rear Crash

The accelerations experienced by the containers in the rear crash were dominated by direct contact. Figure 3-9 compares the x-axis acceleration pulses for the rear container and the vehicle CG for the rear crash. The blue curve is the x-direction acceleration of the vehicle's CG, and the red curve is the x-direction acceleration of the rear container– passenger side accelerometer. The rear container, which is located just beneath the rear bumper, experienced the impact roughly 8 ms sooner than the CG of the vehicle. This is apparent by the red curve rising well before the blue curve. The peak accelerations experienced by the container were also roughly four times higher than the acceleration experienced by the vehicle's CG. This is caused for two reasons, the smaller mass of the containers relative to the entire vehicle, and the direct contact of the billboard on the rear container.
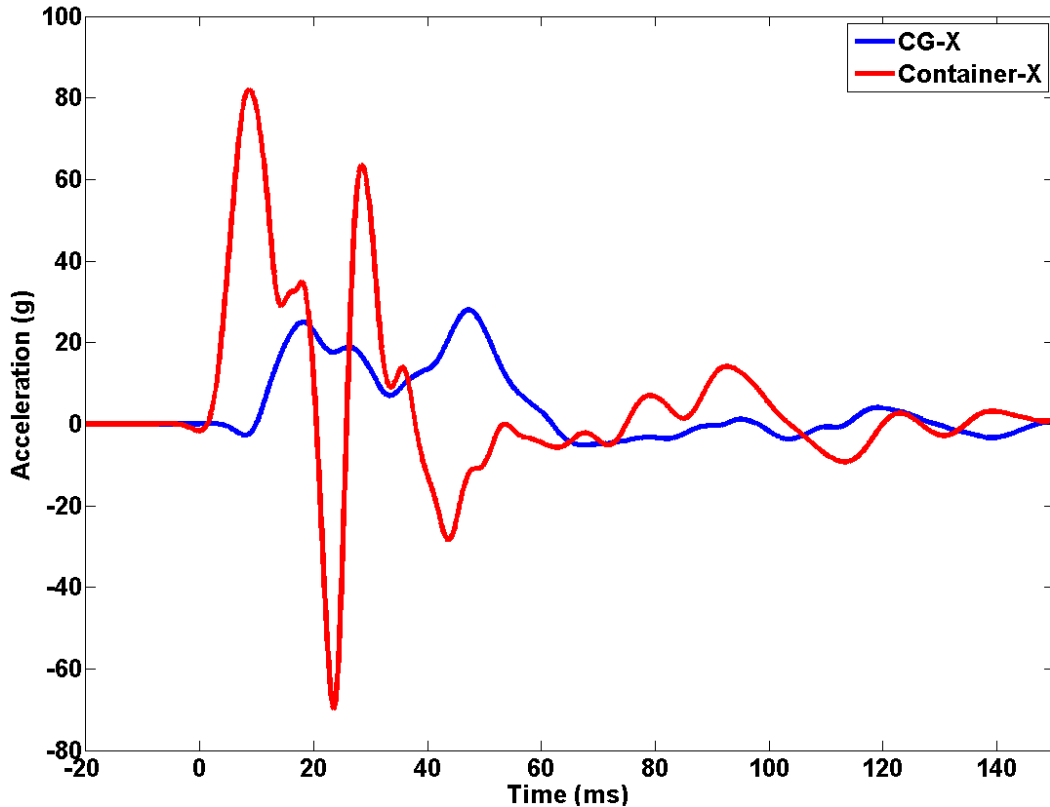
Figure 3-9. X-direction acceleration pulses for the vehicle CG and the rear container (passenger side accelerometer) for the rear crash. The rear container acceleration (red) is substantially higher than the vehicle's CG acceleration (blue).

The peak acceleration experienced by the rear container was approximately 50 percent higher than the peak accelerations experienced by the other two containers. Figure 3-10 compares the x-axis accelerations of all three containers. The initial acceleration of the rear container, shown as the first peak by the green line, was substantially larger than the accelerations of the other two containers. At around 20 ms after the impact, the rear container experienced a negative x-acceleration, while the middle and front containers experienced a positive x-acceleration. This is a result of the rear container pushing a suspension cross member into the middle container. As a result, both the middle container and the front container, which are strapped into the same mounting frame, were pushed forwards. This corroborated with the high-speed pit camera views.
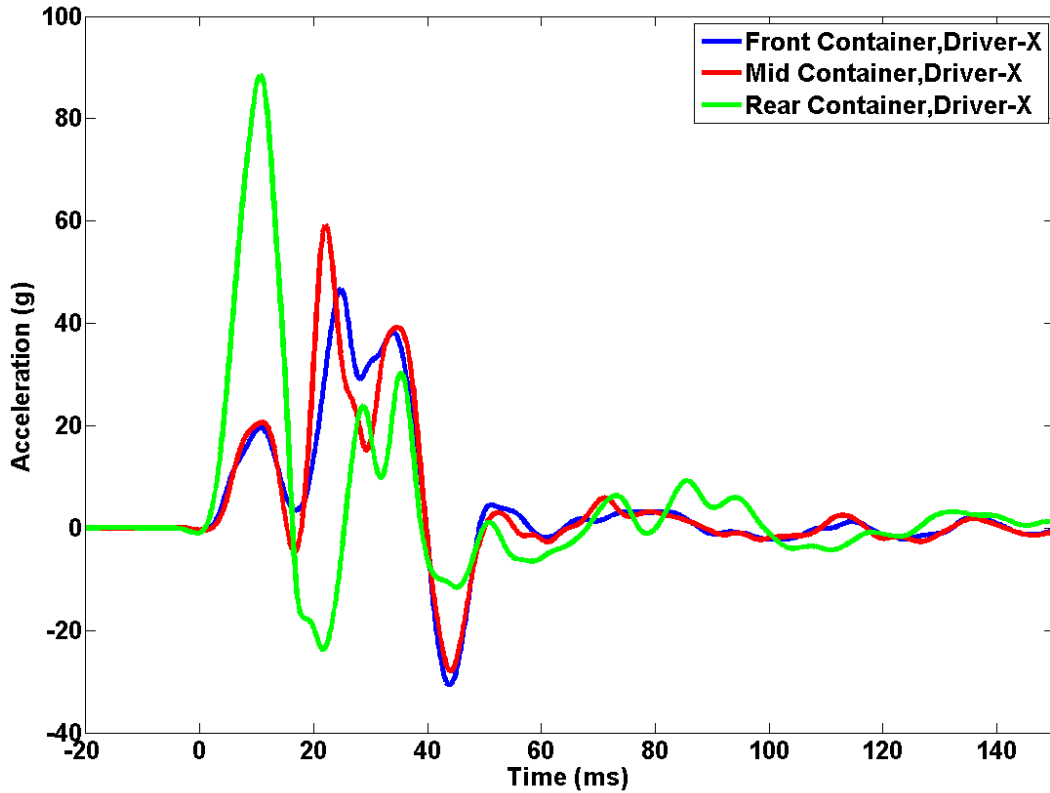
Figure 3-10. X-direction acceleration pulses for the front, middle, and rear containers, driver side accelerometers in the rear crash. The negative acceleration of the rear container (green) coincides with the largest accelerations for the middle (red) and front (blue) containers, which indicates contact between the rear and middle containers.

### 3.3.1.2 Side Crash

In the side crash, the container accelerations were one and a half to two times the vehicle CG acceleration. Figure 3-11 compares the resultant accelerations of the three containers to the vehicle CG resultant. From the figure the peak accelerations are greater the farther the container is located from the CG. This is in part due to the back end of the vehicle swinging around as a result of the impact. Based on the lack of visible damage to the containers and the relatively comparable acceleration levels, the side impact was less severe, to the fuel system, than the rear impact.
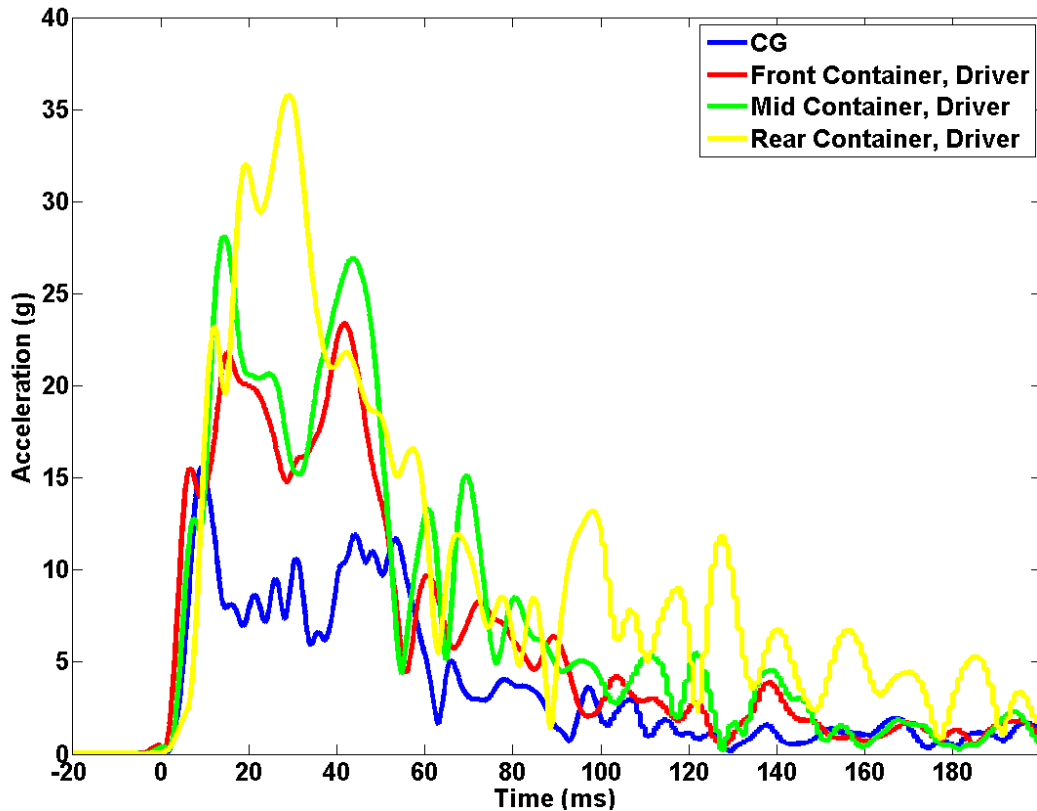
Figure 3-11. Resultant accelerations in the side crash for the vehicle CG (blue) and the driver side accelerations of the front (red), middle (green) and rear (yellow) containers. The peak accelerations are greater on containers farther from the CG.

## 3.3.2 High-Voltage Battery

To reduce the risk of a battery fire, the lithium batteries had been removed from each vehicle prior to the crashes. Ballast was installed in each vehicle to represent the batteries. The original battery housing was sheet steel, 0.85 mm (33.5 mils) thick. Replacement housings were made of 20 gauge steel, 0.91 mm thick (35.9 mils), and a bag of sand weighing 23 kg (50 lb) was put in the housing to approximate the weight of the high-voltage battery assembly. The original vehicle design included a cooling fan that was screwed to the rear face of the battery assembly. The fan assembly sits between the rear cargo door and the battery housing. It was re-installed in the rear crash vehicle so its behavior could be observed. The fan assembly was not re-installed in the side crash vehicle because the threat was not from the rear.

Figure 3-12 shows the remains of the fan assembly following the rear crash. The accelerometers on the passenger side of the compartment recorded a direct impact, which is consistent with the fan assembly being crushed into the battery housing. The original battery housing had vent holes by the fan, but its internal components could easily have been arranged so that cells were unlikely to be punctured by fragments from the fan. The battery housing itself was intact. The resultant acceleration, shown in Figure 3-14, on the driver side of the battery housing was sustained above 20 g for a 50 ms crash pulse and reached a peak of 76 g. The rear crash battery resultant acceleration is much higher than the side crash battery resultant. This is due to the impact from the fan being crushed against the housing in the rear crash.

26
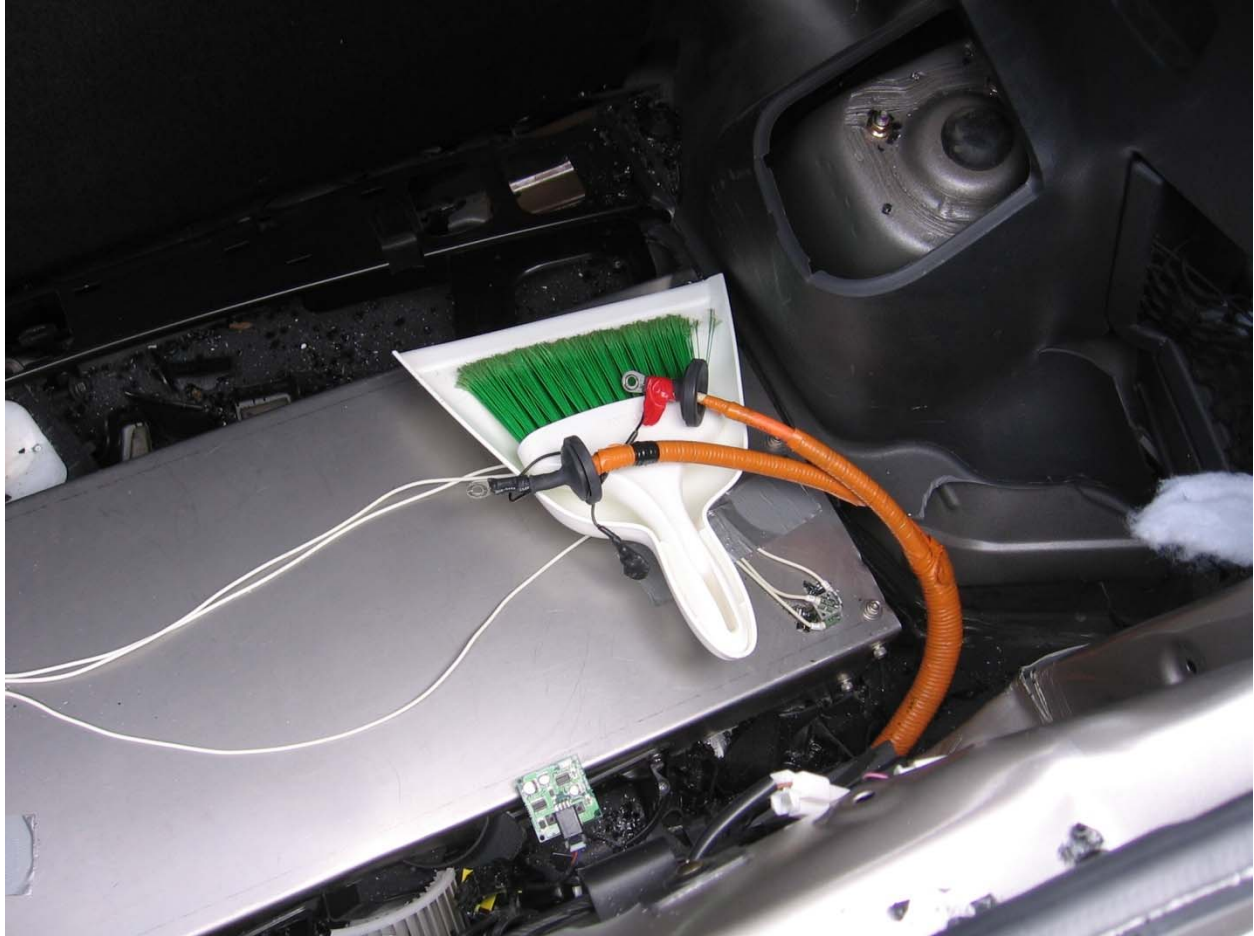
Figure 3-12. The high-voltage battery housing was intact following the rear crash, but the fan assembly was crushed between the rear door and the battery compartment. The white fan itself is visible in the lower left. (The photo was taken during the electrical isolation measurements. The terminals of the battery cable are on a plastic pan to isolate them from the battery housing.)

During the side crash, the resultant acceleration on the driver side of the battery housing was sustained at 15 to 20 g for a duration of 50 ms. The acceleration on the passenger side was sustained for 70 ms and then showed a 60-g impact 100 ms after the crash. Figure 3-13 is a photograph of the replacement battery housing during the post-crash electrical isolation measurements. The mounting platform for a wireless CANLogger was deformed, but the battery housing is essentially intact.

The measured crash pulses can be compared with abuse tests in voluntary standards. Table 3-1 summarizes the specifications of mechanical shock pulses in three battery abuse standards. The pulses can all be represented by a half sine wave of the specified peak amplitude and duration. No published information has been found on the actual behavior of batteries in these tests.
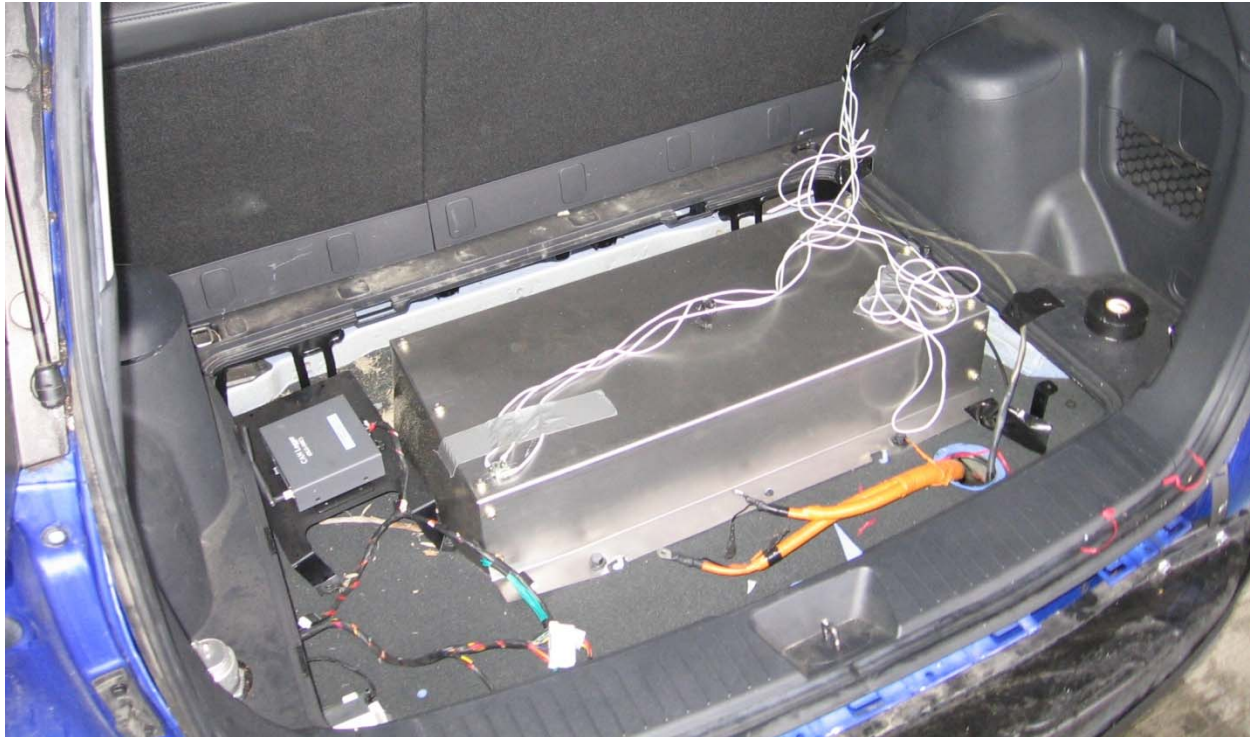
Figure 3-13. The replacement battery housing for the high-voltage battery, shown after the side crash.

Table 3-1. Mechanical shock tests for lithium battery packs in various standards.

| Standard | amplitude | duration | Comments |
|---|---|---|---|
| FreedomCAR [8] Section 3.6 Mechanical Shock, Table 4 | 35 g | 51 ms | The standard explicitly leaves the pulse shape undefined to allow flexibility in testing. The half sine is acceptable. This is the "Mid-1" level. |
| SAE J2464 [26] Section 4.3.1 Shock Tests, Table 4 | 25 g | 15 ms | The standard calls for 18 shocks: 3 axes x 2 directions x 3 repeats. |
| UN [30] 38.3.4.4 Test T.4: Shock | 50 g | 11 ms | This is the pulse for large batteries. The standard calls for 18 shocks: 3 axes x 2 directions x 3 repeats. |

These three idealized pulses are overlaid on the actual crash pulses measured on the driver side of the battery housing in Figure 3-15. These standardized pulses would be applied to the base of a battery under test. The accelerations experienced by the vehicle cross member are representative of the accelerations experienced at the base of the battery housing. The SAE and UN abuse standards call for shocks that are shorter in duration than the pulses in these crashes. The FreedomCAR standard appears to adequately envelope the rear and side crash pulses. A crash test is a single impact (although a crash on the highway may have secondary impacts), and the SAE and UN standards call for repeated impacts. Even so, a component within a battery pack designed to withstand the peak amplitude of one of the standards may fail when subjected to a crash pulse of the amplitude measured here.

The same comparison can be made in the frequency domain. Figure 3-16 shows a shock response spectrum analysis performed on both the side and rear battery resultant accelerations and the three abuse test shock standards. The cross member impacts are fairly well enveloped by the FreedomCAR response spectrum. Typically, in shock response analysis, the accelerations are measured at the base of the object or near a mounting location. As a result the cross member resultants were analyzed in the shock response spectrum, since the cross member acceleration would be a good approximation of the shock input at the base of the battery. The SAE and UN abuse standards do not capture the low frequency responses experienced in the test crashes.
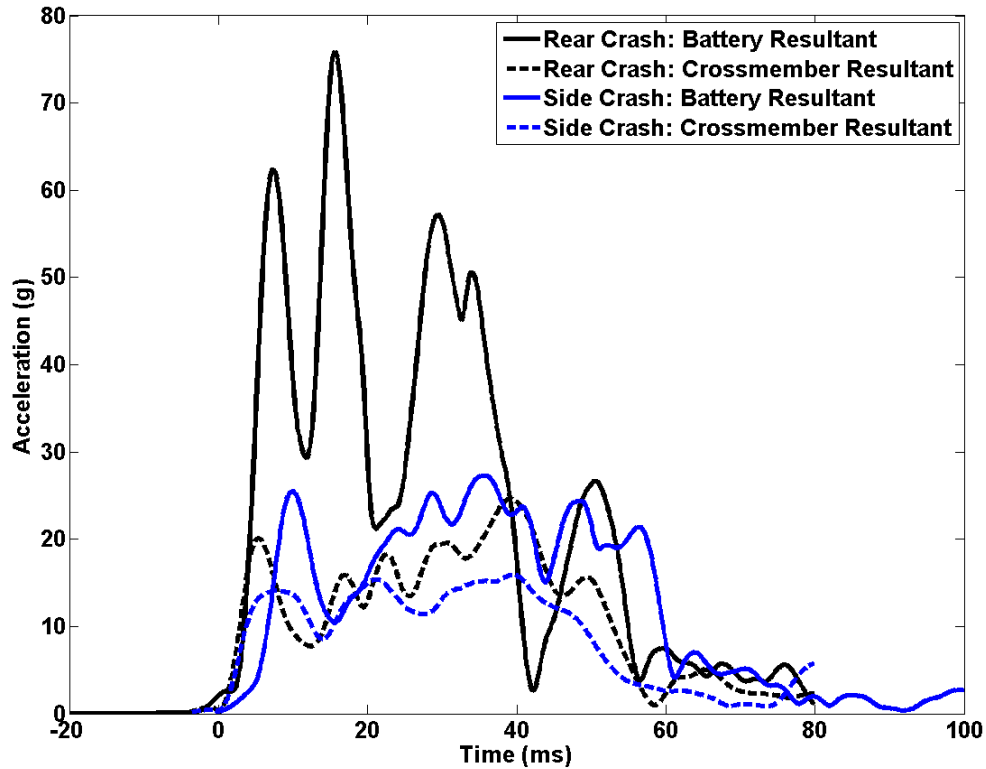


Figure 3-14. Resultant accelerations of the driver side battery accelerometers and the cross member accelerations for both the rear and side impacts. The cross member acceleration is representative of the acceleration that was applied to the base of the battery housing.
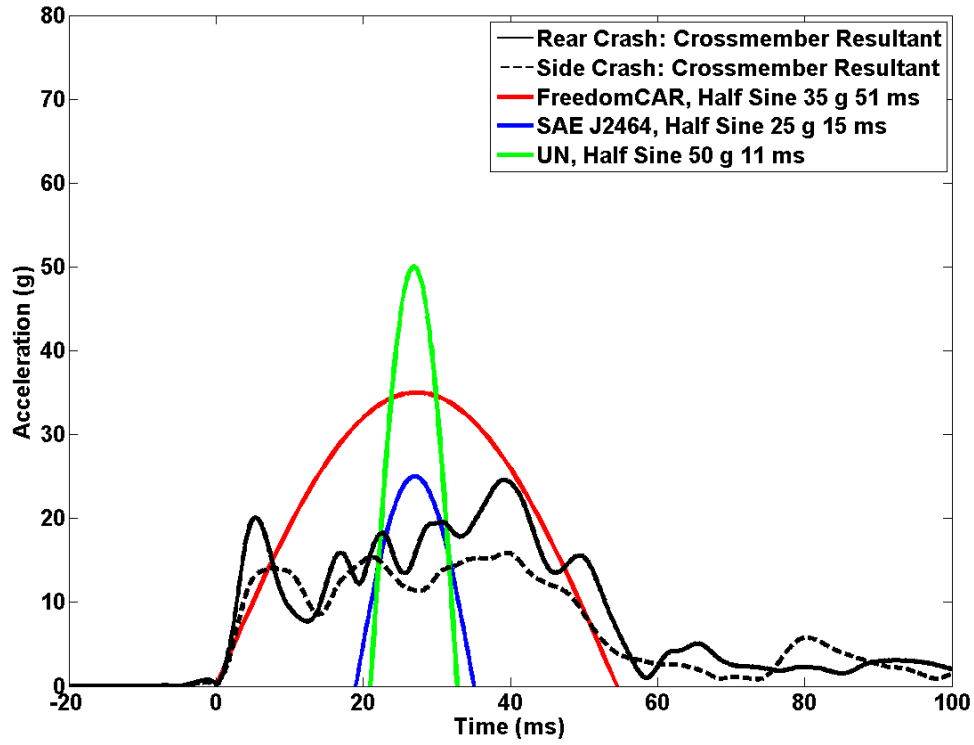
Figure 3-15. Time histories of the rear and side crash acceleration resultants compared with the three lithium battery abuse standards. These two actual crash pulses are a longer duration than the SAE and UN pulses.
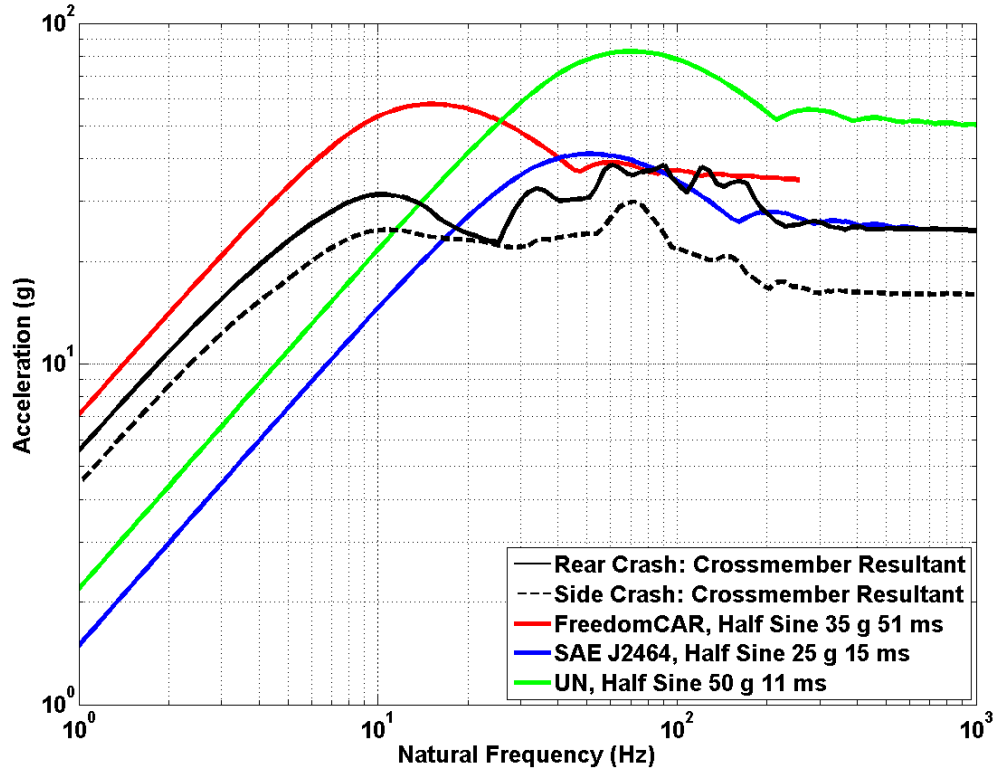
Figure 3-16. Shock response spectrum analysis on the housing for the high-voltage battery in both the rear and side crashes. The shock response spectrums for the three lithium battery abuse standards have been superimposed for reference. The FreedomCAR SRS adequately envelopes the side and rear crashes. The SAE and UN standards are insufficient to capture the lower frequency response of these two crashes.

## 3.4 Pressure Integrity

The fuel systems in both vehicles held pressure following the crashes. Changes in helium density following the crashes were well within the uncertainties of the measurement, so no leak was detected by the pressure drop. The helium sensor mounted near the pressurized container for the side crash detected minute amounts of helium at the moment of the crash and at five instances during the one-hour hold.

### 3.4.1 Pressure, Temperature, and Molar Density

The pressure and temperature of the gas in the fuel container were measured for an hour before and an hour following the side crash. An instrumentation failure stopped the recording several minutes into the hold before the rear crash, so the container was re-pressurized for a second post-crash hold on a later day. In both cases, the quantity of gas in the container was calculated from the pressure, temperature, container volume, and real gas properties.

No measurable helium leak was detected by pressure drop in the fuel system as a result of either the side or the rear crash. This determination was made by examining the ratios of the molar density of helium one hour after the crash to the molar density just before the crash. This ratio,

31

for both crash tests, was indistinguishable from unity, within the limits of the sensors' accuracy. This ratio of unity indicates that there was the same amount of gas in the container after an hour-long hold as at the beginning.

The molar densities were calculated using the NIST's equation of state from the temperatures and pressures recorded during each one hour pressure hold [22]. Error! Not a valid bookmark self-reference. shows the molar density ratios as well as the maximum uncertainties for each crash test.

The pre-crash system leak quantification is of little value since the pressure deviations before the side crash are within the uncertainty of the NIST fluid property model (0.1%) [22]. From the data collected, the pre-crash leak quantification for the rear crash indicated a density increase of 0.3 percent, however this is well within the uncertainty of the instrumentation.

Table 3-2. Results of the pressurization test. A ratio significantly LESS than unity would indicate that gas escaped after the crash.

| Crash Direction | Molar Density Ratio | | Verdict? |
|---|---|---|---|
| | Nominal | Maximum Uncertainty | |
| Rear* | 1.000 | 0.026 | No Leak |
| Side | 0.999 | 0.023 | No Leak |

\* The nominal molar density ratio and max uncertainty based on re-pressurization data

Additional details regarding the uncertainty associated with the gas quantity is analyzed in Appendix F.

## 3.4.2 Helium Sensors

The active fuel system helium sensor on the side crash, located underneath the vehicle, measured a peak of 0.05 percent by volume of helium over a duration of 4 s after the impact. The sensor also recorded several instances of 0.05 percent helium by volume, ranging in duration from one to five seconds, during the one-hour post-crash pressure hold test. The minimum resolution of the detector is 0.05 percent [13]. In this case, if the helium detected were hydrogen, the concentration would have remained well below the lower flammability limit of 4 percent [1]. No helium was measured by the active detector inside the passenger compartment.

After the testing was completed, the helium was vented from the vehicle. During this venting, the fuel system helium detector, on the bottom of the vehicle, measured a peak helium concentration of 8.4 percent over a duration of 230 s. Had the vented helium been hydrogen, the mixture underneath the vehicle would have been well within the flammable range. Over the same period, the passenger compartment helium detector did not measure any helium, despite the windows being open. After the test both helium sensors were verified to be working correctly. This verification was performed by releasing a small amount of helium near the detection point of each sensor and observing the corresponding pulse in the data.

The amount of helium measured by this detector, during the crash and the one hour hold was well below the amount that can be detected by means of a pressure drop. Consequently, sensors of this type may be required to detect very small leaks in hydrogen fuel systems, which may otherwise go unnoticed due to uncertainties in the pressure measurements. However, there is no guarantee that the sensors will always be located in the correct location to detect a leak.

## 3.5    Electrical Isolation

The crashes did not result in measurable differences of electric shock. The differences between pre-crash and post-crash electrical isolation at the various test points on both vehicles were within the measurement accuracy.

All of the test points on both post-crash vehicles, except those on the fuel cell, would have met the unrestricted electrical isolation requirements of FMVSS No. 305, S5.3 of 500 ohms per volt. The 2011 version of this standard permits a lower isolation (100 ohms per volt) for DC voltages on vehicles that monitor isolation. All test points met the lower standard before and after the crash.

As expected, the fuel cell test points had a low isolation even before the crash, which was attributed to the fuel cell being hydrated with aged, conductive water, which could not be flushed from a non-working unit.

Electrical isolation is the ratio of the isolation resistance to the working voltage of the high-voltage source. It is expressed in units of ohms per volt. When the maximum working voltage is the same as the test voltage, the electrical isolation is simply the inverse of the measured leakage current. In performing the calculations, the maximum working voltage of the high-voltage battery was assumed to be 160 Vdc (105% of the specified nominal voltage). Similarly, the maximum working voltage of the fuel cell was assumed to be 480 Vdc (105% of the specified upper nominal voltage).

The isolation measurements at the fuel cell terminals ranged from 174 to 178 ohms per volt, which falls between the two possible lower thresholds of 100 ohms per volt and 500 ohms per volt. Electrical isolation above 500 ohms per volt is required by FMVSS No. 305 for DC high-voltage sources without electrical isolation monitoring during vehicle operation, while at least 100 ohms per volt is required for DC sources when the vehicle implements electrical isolation monitoring during vehicle operation in accordance with the requirements of FMVSS No. 305 S5.4. The lower threshold for all AC sources is 500 ohms per volt.

To minimize the risk of a battery fire the high-voltage battery had been removed and replaced with ballast. Had the battery been in place, deformation of the enclosure could have reduced the electrical isolation. A factor that could have affected fuel cell isolation results is that the coolant pumps in these inoperable vehicles could not be started, and thus the coolant loop could not be fully cycled. The vehicles in these crash tests had not been operated in more than a year before the crashes. Whether the fuel cell was fully hydrated, partially hydrated, or dry could not be determined without the ability to flush the coolant. A dry fuel cell would have resulted in a high isolation, so the fuel cell was likely either fully or partially hydrated with aged, conductive water. The coolant could not be flushed and replaced with fresh deionized water before the crashes. Therefore, the isolation that was measured between the fuel cell and the chassis is less than what would be expected in a recently operated and well maintained vehicle. Also, without the battery present, this result does not account for any breach in isolation that could have occurred within the high-voltage battery pack.

Results of the measurements are in Table 3-3 and Table 3-4. Refer to appendix A, Electrical Isolation Measurments, for details on Quadtech Gaurdian 5000 safety analyzer.

Table 3-3. Electrical isolation measured before and after the rear crash.

| Test Point | Isolation, Ohms per Volt | | |
| --- | --- | --- | --- |
| | Pre-Impact | Post-Impact | Change |
| HV Battery + | 2900 ± 500 | 2700 ± 400 | -200 |
| HV Battery - | 2800 ± 400 | 2700 ± 400 | -100 |
| Fuel Cell + | 177 ± 5 | 177 ± 5 | 0 |
| Fuel Cell - | 177 ± 5 | 176 ± 5 | -1 |
| MCU DC + | 883 ± 51 | 883 ± 51 | 0 |
| MCU DC - | 868 ± 50 | 883 ± 51 | +15 |
| MCU AC-1 | 887 ± 51 | 883 ± 51 | -4 |
| MCU AC-2 | 887 ± 51 | 883 ± 51 | -4 |
| MCU AC-3 | 887 ± 51 | 883 ± 51 | -4 |

Table 3-4. Electrical isolation measured before and after the side crash.

| Test Point | Isolation, Ohms per Volt | | |
| --- | --- | --- | --- |
| | Pre-Impact | Post-Impact | Change |
| HV Battery + | 2900 ± 500 | 2800 ± 400 | -100 |
| HV Battery - | 2800 ± 400 | 2800 ± 400 | 0 |
| Fuel Cell + | 175 ± 5 | 178 ± 5 | +3 |
| Fuel Cell - | 174 ± 5 | 178 ± 5 | +4 |
| MCU DC + | 895 ± 52 | 895 ± 52 | 0 |
| MCU DC - | 895 ± 52 | 891 ± 52 | -4 |
| MCU AC-1 | 895 ± 52 | 891 ± 52 | -4 |
| MCU AC-2 | 895 ± 52 | 891 ± 52 | -4 |
| MCU AC-3 | 895 ± 52 | 891 ± 52 | -4 |

# 4.0 CONCLUSIONS

Two prototype hydrogen fuel cell vehicles were crashed in this task order. Measurements were collected to identify the consequences on the fuel system and electrical system. The purpose of this task order was to provide NHTSA with data from realistic crashes on hydrogen fuel cell vehicles, to aid in their development of possible regulations and compliance test procedures. Observations of the crashes, and their implications on vehicle design and future testing, are covered in this section.

## 4.1 Implications for Vehicle Design

The integrity of the fuel and electrical systems for these two prototype vehicles held. Demonstrating that these particular and built fuel cell vehicle withstood the conditions of these two research tests.

### 4.1.1 Integrity and Vulnerabilities of the Fuel System

The tests proved to be a challenge to the fuel system. However fuel system integrity can be achieved through the use of quality components and designed vehicle safety systems, such as crumple zones. Results from this research were that the vehicle worked as a system to protect the container and other fuel system components. Even with the vehicle's protection, it is possible for the fuel system to sustain damage. Deformation of tubing and surface damage on containers was observed in the rear crash test.

The rear crash displaced all three containers from their original location. The rear container was directly impacted by the billboard barrier and pushed forward into a suspension cross member. This cross member, under the force from the rear container, was pushed forward and impacted the middle container. The front container which shared a mounting bracket with the middle container was also displaced towards the front of the vehicle and sustained a small gouge in the dome from contact with the vehicle underbody.

Thick walled stainless steel lines proved quite robust and deformed under load while maintaining pressure integrity. Ductile tubing and high-quality fittings are essential.

### 4.1.2 Integrity and Vulnerabilities of the Electrical Isolation

The electrical isolation measured in these vehicles was the same after the crashes as it was before. However, certain hazards are undetectable by present methods.

One hazard that could have been undetected is a breach in the coolant loop causing a conducting path between the fuel cell terminals and the electrical chassis. The breach would be undetected because the conducting path would exist on the high-voltage source side of the automatic disconnects, while FMVSS No. 305 specifies that the measurements be performed on the power train side of the automatic disconnects if the disconnect is physically contained within the high-voltage source. The isolation between a fuel cell terminal and the electrical chassis could be much lower than the isolation between the power train side of the automatic disconnect and the electrical chassis.

An alternative or supplementary approach may be an on-board system that automatically monitors isolation at the high-voltage source side of the automatic disconnects and displays a warning for loss of isolation or loss of the monitoring system's readiness.

# 4.2    Implications for Future Tests

The behavior of the vehicle itself in FMVSS No. 301 crashes is well documented through the many compliance tests run by NHTSA, whose results are published [20]. These crashes focused on the structural behavior of the fuel systems—the container, its mounting, and the associated piping—and the electrical isolation.

## 4.2.1  Crash Conditions

The purpose of the full-vehicle crash tests was to demonstrate the behavior of a hydrogen container and its mounting in a crash test. Accelerations and deformations were measured to quantify the conditions endured by the test vehicle and more importantly, by the containers during a crash test. These crash tests, based on existing FMVSS, proved to be reasonable challenges to these prototype hydrogen fuel systems.

The crash pulses measured at the housing for the high-voltage battery are higher than those specified for mechanical shock in existing battery abuse test standards.

## 4.2.2  Contents and Pressurization Options

Existing crash tests for fuel system safety call for the fuel to be removed and replaced with a non-combustible simulant. How to fill a compressed hydrogen fuel system for a crash test is not a simple question. The various options for both the material and the pressure have advantages and disadvantages.

### 4.2.2.1  Discussion of Test Gas Options

Pure gases of nitrogen, helium, and hydrogen have disadvantages of detectability, availability, and safety, respectively. Originally the test gas to be used in these tests was to be helium, at 100 percent of service pressure for the side crash, and 10 percent service pressure in the rear crash. However, helium proved to be an expensive option for pressurizing to 100 percent fill, so a mixture of 80 percent helium and 20 percent nitrogen was used for the side crash test. A calibrated mixture of mostly nitrogen with either hydrogen or helium should be considered to monitor container pressure, while allowing for detection of low level helium or hydrogen leaks in and around the vehicle using gas sensors such as those provided by NREL for these tests.

Nitrogen

Nitrogen, as for a CNG test in FMVSS No. 303, is not flammable, but $N_2$ molecules are much larger than $H_2$ molecules and will not leak through minuscule passages through which hydrogen could pass. A second disadvantage of nitrogen is that a small amount of leaked nitrogen could not be sensed outside the container because most of the atmosphere is nitrogen. Nitrogen would serve to stress the components and detect gross leaks by a pressure drop, but is not the most appropriate fill gas for testing a hydrogen fuel system.

## Helium

Helium's properties may be ideal for leak detection, but have other considerations. The gas is commonly used for leak detection in scientific instruments where all leaks must be avoided because its molecule, only a single atom, is small and because inexpensive instruments are available to detect it in trace quantities. Its disadvantage is its cost and availability. Helium cannot be manufactured; it can only be gathered, and the worldwide supply is limited. Some suppliers of compressed gas are not accepting new customers for helium. A plan to highly pressurize fuel systems with helium would be unsustainable in the long term. Buying pure helium to test at only 10 percent of service pressure might be workable.

## Hydrogen

Hydrogen, presumably the gas in the fuel system when the vehicle is purchased, would leak more readily than nitrogen and can be detected in trace quantities well below its lower flammability limit. If the crash test is presumed to be a success, hydrogen has much to recommend it. However, precautions would always have to be taken for a failed test and for the handling and disposal of the damaged, but full components, following the test. Recall that, when the fuel container was vented following the successful side crash, the concentration of test gas under the vehicle was measured to be in the range of what would have been a flammable mixture for hydrogen.

## Gas Mixtures

Standard gas mixtures such as 5 percent helium with balance of nitrogen, and 5 percent hydrogen, balance nitrogen, are available pre-mixed from most industrial gas suppliers. These gas mixtures are typically used in leak detection applications as a less costly alternative to using pure helium. Of course, when the helium or hydrogen is diluted, it will leak in lesser amounts and not be as readily detectable. The necessary minimum fraction of trace gas would depend not only on the tolerable leak, but the volume of the passenger compartment. Custom blends of gasses can be ordered. A mixture of more than 5 percent hydrogen would risk being flammable; a mixture of more than 5 percent helium would be expensive. Furthermore, not all industrial gas suppliers can provide both mixtures in a 6K bottle size. In situations where high pressure mixed gas bottles are not available, a gas intensifier may be required to reach pressures above 156 bar (2,262 psi). A "Certified Standard" mixture would have adequate tolerance and is less expensive than the "Primary Standard." While a mixed gas approach may not be as ideal as using 100 percent helium, a mixture is a suitable compromise between cost, availability, and leak detection characteristics.

The equation of state calculations necessary for calculating a leaked mass from a pressure and temperature change would be via a mixed gas property calculator such as NIST's REFPROP computer program [21].

## Order-of-Magnitude Costs

Table 4-1. List Price for a bottle of
potential fill gases

| Gas | Unit List Price* | Nominal Bottle Pressure |
|---|---|---|
| Helium | $1,100 | 6,000 psi |
| Hydrogen | $300 | 6,000 psi |
| Nitrogen | $280 | 6,000 psi |
| 5% He, Balance $N_2$ | $980 | 6,000 psi |
| 5% $H_2$, Balance $N_2$ | $440 | 2,300 psi |
| 5% He, Balance $N_2$ | $460 | 2,300 psi |
| *List price current as of 2012 | | |

The selection of gas can have a considerable effect on the cost of a crash test, particularly if an entire fuel system is to be fully pressurized.

Battelle asked two major suppliers of compressed gas for list prices that could be included in this report. The average of the two prices for "6k" (6,000 psi) bottles and "k" (2,300 psi) bottles of the gases are in Table 4-1. Regular customers would have volume discounts, and bottle rental is ignored.

To limit the consequences of a fuel system failure during the crash tests, the fuel system in these crashes was modified so that only one of the containers would be pressurized. Presumably, an eventual compliance test would test the entire fuel system and all containers in a multi-container vehicle would be pressurized. Taking the full volume of the test vehicles' fuel systems—152 L— as a typical capacity of a hydrogen fuel system, a single bottle would be sufficient to fill the system to 10 percent of service pressure. Pressurizing to full service pressure using bottles would require an intensifier—capital equipment that essentially pumps the gas from the bottle to the vehicle—or a cascading process, where bottles are sequentially connected to the fuel system until the desired pressure is reached. If the cascading method is used, approximately 8 bottles of each gas would be needed to bring a 152 L system to 350 bar. That is, the cost of gas for a compliance test would be 8 times the price listed in the table.

A Word on Safety

When removing hydrogen from a container to fill with another gas, avoiding a flammable mixture within the container is paramount. Oxygen in any form, including air, must be kept out of the container until the hydrogen is thoroughly removed. If oxygen and a fuel are in the container at the same time, the slightest ignition source can rupture the container. Even after the pressure has been released from a fuel container, hydrogen at atmospheric pressure remains and must be removed with care.

## 4.2.2.2 Test Pressure

In these crash tests and in the previous three tests conducted under Task Order 1, different container fill pressures were used for side impacts than for front and rear impact tests. In frontal and rear impacts, where transversely mounted containers were impacted on their sides, the containers were filled to 10 percent of service pressure. The crush tests of Task Order 1 demonstrated more circumferental deformation of side-impacted containers when they were filled to 10 percent of service pressure than 100 percent of service pressure. Lower pressure provides less stiffening of the container walls than does higher pressure, allowing more flexure and deformation upon impact.

In vehicle side impact crashes where the end mounted valves could have been impacted, the containers were filled to 100 percent of service pressure. The crush tests on container domes of Task Order 1 caused more damage to fully pressurized containers than to nearly empty containers. The fill pressures selected for these experiments were considered worst case for the direction of impact relative to the container orientation. Despite testing under worst case conditions, there was no indication in the vehicle crash tests that the containers were impacted sufficiently to induce failure.

Assessment of the results suggests that a lower pressure, such as 10 percent of service pressure may be the most appropriate for all crash tests. Container crush tests in Task Order 1 indicate that it is very unlikely that a hydrogen fuel container will fail or leak in a vehicle crash. The impact necessary to cause failure of a container is well beyond what a container, protected and mounted, inside a vehicle can experience in even severe crashes.

Although a container is unlikely to fail, it can flex circumferentially and in the dome if impacted during a crash. Flexure may damage composites in the container. For a given impact, flexure will be greater at lower internal pressures due to the lesser stiffness. While the damage is likely not enough to cause immediate failure, it could contribute to delayed failure if the container were to continue in service and be refueled many times.

Consequently, this logic suggests that a lower pressure be used for fuel containers during a crash test and that the fuel containers be inspected for evidence of damage following the test.

## 4.2.3 Detection of Leaks

In Task Order 3, hydrogen was leaked into the passenger compartment, trunk, and underneath the vehicle at various rates (3 to 236 LPM). An array of sensors was used to measure hydrogen concentration at several locations inside the vehicle for the matrix of leak rates and durations. That Task Order concluded that:

> "With regard to achieving the objective of determining a minimum allowable post-crash leak rate, test data indicate that leak rate is not the most important metric, but the volume of hydrogen leaked into car compartments to accumulate locally to ~5%, a level just exceeding the lower flammability limit of hydrogen, ~4%. It appears unimportant whether this lower flammability limit is reached via a low leak rate after a long duration (up to 60 m) or via a high leak rate (up to 118 lpm) after a very short duration."

Two complementary means of detecting leaks should be implemented for hydrogen fuel cell compliance testing. The first means of detecting a leak is through monitoring the pressure of the fuel system, and checking for evidence of a pressure drop. The second way to detect a leak during the crash test is by using sensors to detect a tracer gas which may have escaped the fuel system boundary. Each method has its shortcomings; however, if both methods are used simultaneously, a reasonable conclusion of whether or not a dangerous leak was present can be obtained.

## 4.2.3.1 Detection of Leaks by Pressure Drop

The first means of detecting a leak during testing is by measuring the temperature and pressure of the gas inside the fuel container prior to the crash, and at some specified time after the crash. These measurements can then be input into a fluid equations-of-state model to calculate the amount of fuel present in the system. In theory, if the amount of fuel present before the crash is equal to the amount of fuel after the crash, then no leak was present.

However, this method of leak detection is limited by inherent uncertainty in the temperature and pressure measurements, as well as some uncertainty in the fluid's equation of state and composition. As a result of these uncertainties, there is a minimum detectable leak threshold, below which no definitive conclusion of a leak can be made.

The amount of hydrogen required to reach a concentration exceeding the lower flammability limit (LFL) of 4 percent is low compared to the amount in a pressurized container. For example, the size of a typical passenger compartment is on the order of 2800 L (100 ft$^3$). If spread uniformly throughout this volume, the amount of hydrogen required to raise the concentration to the LFL is 4.9 moles.[1] The amount of hydrogen present in a 152-L fuel system, at 350 bar (5,076 psi) and 20 C is roughly 1,800 moles. Therefore, the loss of 4.9 moles would reduce the system pressure by only 1.18 bar (17 psi), or 0.34 percent. For 10 percent of service pressure, the reduction in system pressure as a result of a 4.9-mole loss would be 0.83 bar (12 psi), a more readily detectible 2.4-percent drop in pressure.

---

[1] Density of expanded hydrogen taken at NTP, 293.16K and 1.013 bar (14.7 psia)

If a compliance test were run at 10 percent of service pressure, the OEM pressure transducer would have to be changed to a more sensitive transducer. This would result in breaking the pressure boundary of the vehicle to install the pressure transducer.

Unfortunately, calibration-quality pressure transducers, with accuracies better than 0.02 percent full scale, are not currently rated for the mechanical shock levels above a few g and are not expected to survive crash testing.

While the pressure drop detection method may not be practical for detecting a small leak, it will provide positive detection of a gross leak. It can provide an upper bound on the size of a leak. The advantages and disadvantages of detecting leaks by measuring pressure are summarized in Table 4-2.

Table 4-2. Pros and cons of the pressure drop leak detection method.

| Pros | Cons |
|---|---|
| <ul><li>Independent of the type of gas used in the test.</li><li>A 'big picture' look at the amount of mass in the fuel system.</li><li>Could be used to quantify the size of a large leak.</li></ul> | <ul><li>Practical limitations on the minimum detectable leak size.</li><li>Uncertainty highly dependent on instrumentation used.</li><li>Good experimental and analysis practices are required for meaningful data.</li></ul> |

## 4.2.3.2 Detection of Leaks Using External Sensors

The second method that should be employed to detect leaks during a compliance test is sensors mounted inside the passenger compartment and around major fuel system components.

The hydrogen and helium detectors used for this project measure thermal conductivity. Hydrogen and helium have a thermal conductivity that is significantly different from that of air. Around room temperature, hydrogen, helium and neon have the largest thermal conductivity differences compared to air. Since air is mostly nitrogen, the thermal conductivity of pure nitrogen gas is almost identical to that of air. Table 4-3 lists the ratio of thermal conductivities of several gases compared to that of air. The use of standard gas mixtures (5% helium or hydrogen, balanced with nitrogen) is a suitable compromise to using pure helium gas.

Table 4-3. Comparisons with air of the thermal conductivities of several gases.

| Gas | Ratio of thermal conductivity of the gas to air (at 26.7 C)[6] |
|---|---|
| Air | 1.000 |
| Nitrogen | 1.003 |
| Hydrogen | 7.175 |
| Helium | 5.794 |
| Neon | 1.860 |

The results from Task Order 3 indicated that if hydrogen were detected in the passenger compartment (even below the lower flammability limit of 4%), passengers are in jeopardy. This is because the sensor detects the concentration of hydrogen at a single point, which does not guarantee there is not a more concentrated pocket somewhere else in the vehicle, which is of high probability as indicated by extensive hydrogen accumulation tests. As such the report concluded, "All accumulation of hydrogen should be avoided in passenger compartments." Thus, any tracer gas detected inside the passenger compartment would indicate a hazardous

condition. One observation from Task Order 3 was the presence of a scorch mark on the headliner. Therefore, sensors inside the passenger compartment should be mounted as close to the sheet metal roof as possible. A gap between the fabric headliner and the sheet metal roof is usually filled with insulation or air. As such, the fabric headliner is a 'faux' barrier, which still allows for the permeation of hydrogen, possibly resulting in hydrogen accumulation above the headliner. Removal of the headliner to allow for proper mounting of the sensors may be required.

Another consideration is the use of a continuous air exchange system that monitors the air coming out of the passenger compartment for hydrogen. Depending on the detector used, some engineering considerations may need to be made to keep moisture from affecting the hydrogen detectors. Not all hydrogen detectors are affected by the moisture content in the air. The advantages and disadvantages of detecting leaks using gas sensors are summarized in Table 4-4.

Table 4-4. Pros and cons of leak detection using gas sensors.

| Pros | Cons |
| --- | --- |
| • Can be used to detect the presence of a tracer gas inside the passenger compartment or around fittings.<br>• Can detect much smaller leaks than by means of the pressure drop method. | • Thermal conductivity of the gas must be sufficiently different than air for detection.<br>• Sensor must be in the right location to detect a leak.<br>• Difficult to quantify the size of the leak.<br>• Will not work with nitrogen. |

## 4.2.4 Detection of Breaches to the Electrical Isolation

Battery isolation can be measured using a voltmeter and the process described in FMVSS No. 305 (2011), similar to other battery-powered electric vehicles. The high-voltage sources in these prototype crash tests were removed to minimize the risk of battery fire in the event of a breach to the lithium battery. This may not be required for eventual compliance tests. In other electric vehicle testing, the high-voltage battery is installed and active.

Tetsting would be more complete and more realistic with the fuel cell active and current circulating. This would providing realistic thermal conditions and allow isolation measurements to be performed with a voltmeter, as is done for other high-voltage sources. With the fuel cell inactive, a testing device such as a safety analyzer would be necessary for isolation measurements. As part of the Electrical Isolation Task Order 4, testing showed the effective isolation resistance of a sample of Glysantin decreased approximately by a factor of four when temperature was increased from 25° C to 100° C, as shown in Figure 4-1. Thus, temperature of the vehicle will significantly affect fuel cell isolation. If the fuel cell cannot be active due to the inability to use hydrogen, temperature correction factors for different types of coolant will need to be developed.
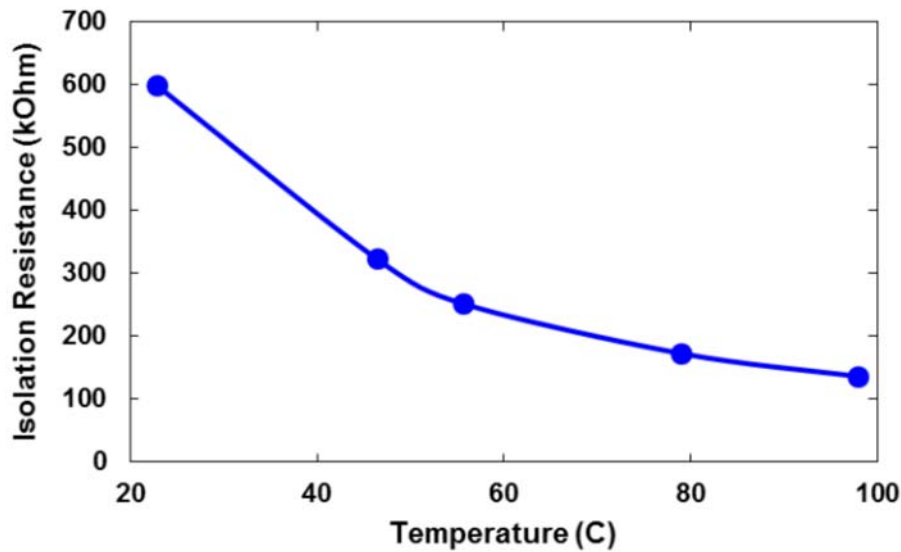
Figure 4-1. The resistivity of Glysantin decreases with increasing temperature. Data from Task Order 4.

The isolation between the fuel cell and the chassis depends on the conductivity of the coolant if the coolant is not electrically isolated from the chassis. Fresh deionized water has a low conductivity and gives good isolation. As coolant ages, either by sitting or by running, the water gradually gathers impurities that increase its conductivity. A fuel cell with aged, ionized (conductive) coolant is not as well isolated from the chassis unless the vehicle utilizes an ion exchange resin filter to maintain low coolant conductivity. Because the measurement of isolation depends on the quality of the coolant, the coolant must be specified for a measurement to be meaningful.

Ideally, the test would examine the worst case (highest coolant conductivity scenario), to ensure that safety is maintained over the course of normal vehicle operation. If this is not feasible, correction factors may need to be developed. Determining worst case conditions involves knowing the type of coolant and its temperature versus conductivity profile, the manufacturer's shelf life data, whether the vehicle uses an ion exchange resin filter, the manufacturer's longest recommended period before filter replacement, and the manufacturer's recommended frequency of coolant replacement or addition. Requiring that the coolant be in the worst case condition may result in a more expensive process, but would produce results at the manufacturer's designed limits. Applying a correction factor to estimate the worst case condition would be less expensive, but the results may be less accurate.

# 5.0 OVERALL CONCLUSIONS AND RECOMMENDATIONS

The fuel cell vehicles crashed in this study require examination in two ways that are not common in current vehicles—the hydrogen containers and isolation of the high voltage. Conclusions were drawn in both areas.

## 5.1 Leak Detection

Detecting minute leaks by monitoring the pressure drop is not likely practical. Uncertainty in the pressure and temperature measurements is likely to be greater than any perceived loss in the amount of hydrogen or helium as a result of the crashes. This was true in Task Order 1, where CNG vehicles were retrofitted with hydrogen containers and tested with hydrogen as the fill gas, and in this task, where retired fuel cell vehicles were tesed with helium or a mix of helium and nitrogen. This does not imply that the temperature and pressure should not be monitored. Both temperature and pressure data should be collected throughout the crash and the post crash monitoring period, as it is beneficial in bounding the size of the potential leak. Uncertainty analysis is critical for determining the minimum detectable leak size.

One finding from Task Order 3, which assessed the safety of post-crash hydrogen leaks in and around vehicles, was that the tolerable leakage of hydrogen inside a vehicle should be less than the amount required to bring the hydrogen concentration of the passenger compartment volume up to 4 percent. This amount is small relative to the amount contained in a fully pressurized fuel system. Any accumulation of hydrogen in the passenger compartment is potentially dangerous. This result shows the importance of having hydrogen or helium sensors in the passenger compartment as well as near fuel system components that have the potential for leaking as a result of the crash. Sensors, such as those used in this experiment would detect the presence of any hydrogen during the crash or post-crash hold. These sensors will aid in determining if any hydrogen could have entered the passenger compartment after the crash.

For the successful use of these sensors, a detectable gas such as helium must be used in the compliance test. Pure helium is one potential fueling option; however, there are advantages to using standard gas mixtures, such as 5 percent helium, balance nitrogen.

In realistic crashes, where the fuel container is protected within a vehicle, its greatest chance of damage is flexing in its wall. This is most likely to happen when the container is at low pressure—nearly empty. This is true for all impact orientations. One crash each in Task Orders 1 and 7 were conducted with the container fully pressurized because that is the most vulnerable condition for severe longitudinal impacts. In both of these experimental crashes, the vehicle adequately protected the container; in fact, the container itself was not directly impacted in either crash. A similar but slightly more severe crash would cause a nearly empty container to deform. Therefore, the lower pressure can be considered the worst case test condition.

## 5.2  Electrical Isolation

The risk of electric shock did not increase as a result of the crash tests performed under Task Order 7. Based on the FMVSS 305 S5.3 procedures, all test points for both crashes would have met the electrical isolation requirements. In these tests, the high-voltage batteries were removed to minimize the risk of a battery fire. As a result, the electrical isolation measured in this study do not account for a potential breach that may have occurred within the high-voltage battery.

The side impact shock response experienced by the high-voltage battery is comparable to the shock abuse test recommended in the FreedomCAR standard. The other two shock abuse standards do not adequately envelope the range of frequencies prevalent in a realistic shock event. The rear impact shock response was much higher than even the FreedomCAR standard. This is likely a result of the direct impingement of a cooling fan that was crushed between the battery housing and the trunk wall as the crumple zone was compressed.

# 6.0 REFERENCES

1. Air Products. (Revised April 2006). Hydrogen Material Safety Data Sheet. (MSDS Number 300000000074). Available online at https://apdirect.airproducts.com/msds/DisplayPDF.aspx?docid=63578

2. Flamberg, S., Rose, S., & Stephens, D. (2010, February) Analysis of published hydrogen vehicle and safety research. (Project Report for Contract No. DTNH22-08-D-00080 Task Order 5. Report No. DOT HS 811 267). Washington, DC: National Highway Traffic Safety Administration. Available at www.nhtsa.gov/DOT/NHTSA/NVS/Crashworthiness/Alternative%20Energy%20Vehicle%20Systems%20Safety%20Research/811267.pdf

3. Battelle Memorial Institute. (March 24, 2010). Electrical isolation test procedure development and verification. (Project Report for Contract No. DTNH22-08-D-00080 Task Order 4). Columbus, OH: Author.

4. Battelle Memorial Institute. (May 5, 2010) Post-crash hydrogen leakage limits and fire safety research. (Draft Project Report for Contract No. DTNH22-08-D-00080 Task Order 3). Columbus, OH: Author.

5. Battelle Memorial Institute. (April 1, 2011) Compressed Hydrogen Container Fuel Options for Crash Testing. (Draft Final Report to the National Highway Traffic Safety Administration on Contract No. DTNH22-08-D-00080 Task Order 1). Columbus, OH: Author.

6. Weast, R. C., & Astle, M. J. (eds.). (1983).CRC Handbook of Chemistry and Physics, 64th Edition. Boca Raton, FL: CRC Press. ISBN 0-8493-0464-4.

7. 49 CFR 587 – Deformable Barriers , Subpart B – Side Impact Moving Deformable Barrier. http://frwebgate.access.gpo.gov/cgi-bin/get-cfr.cgi?TITLE=49&PART=587&SUBPART=b&TYPE=PDF

8. Doughty, D. H., & Crafts, C. C. (2006) FreedomCAR electrical energy storage system abuse test manual for electric and hybrid electric vehicle applications. (Sandia Report SAND2005-3123). Albuquerque, NM: Sandia National Laboratories. . Available at http://prod.sandia.gov/techlib/access-control.cgi/2005/053123.pdf.

9. ECE/TRANS/WP.29/GRSP/2012/23. (2012, September 25). Revised draft global technical regulation on hydrogen and fuel cell vehicles. Geneva: United Nations Economic Commission for Europe. Available at www.unece.org/fileadmin/DAM/trans/doc/2012/wp29grsp/ECE-TRANS-WP29-GRSP-2012-23e.pdf

10. 49 CFR Part 571. Federal Motor Vehicle Safety Standard No. 301; Fuel system integrity. (Docket No. NHTSA-00-8248, RIN 2127-AF36). Available at http://www.nhtsa.gov/cars/rules/rulings/301nprm/index.html

11. 49 CFR 571.393. Federal Motor Vehicle Safety Standard No. 303; Fuel system integrity of compressed natural gas vehicles.
Available at http://ecfr.gpoaccess.gov/cgi/t/text/text-idx?c=ecfr&sid=6b6c68347b9728d911cf1e067ddec2e0&rgn=div8&view=text&node=49:6.1.2.3.37.2.7.66&idno=49

12. 49 CFR 571.305. Federal Motor Vehicle Safety Standard No. 305; Electric-powered vehicles: electrolyte spillage and electrical shock protection.
Available at http://ecfr.gpoaccess.gov/cgi/t/text/text-idx?c=ecfr&sid=53da96b665086e88988521c11b21fb4b&rgn=div8&view=text&node=49:6.1.2.3.39.2.7.69&idno=49

13. AppliedSensor. (2008). Automotive hydrogen safety sensor manual. (HSS-440P, Revision PA4). Reutlingen, Germany: Author.

14. Motor Vehicle Standards and Research Branch, Road Safety and Motor Vehicle Regulation Directorate. (2001, February 8). LPG Fuel System Integrity, Test Method 301.1. Ottowa: Transport Canada.

15. McDougall, M., & Stephens, D. (2013, August). Cumulative fuel system life cycle and durability testing of hydrogen containers. (Report No. DOT HS 811 832). Washington, DC: National Highway Traffic Safety Administration.) Available at www.nhtsa.gov/DOT/NHTSA/NVS/Crashworthiness/Alternative%20Energy%20Vehicle%20Systems%20Safety%20Research/811832.pdf

16. NHTSA. (2007, January 17). Laboratory Test Procedure TP-301-04. Fuel system integrity – Frontal fixed barrier impacts, standard regulation on fuel system integrity – Frontal fixed barrier impacts. Washington, DC: Author. Available at www.nhtsa.gov/DOT/NHTSA/Vehicle%20Safety/Test%20Procedures/Associated%20Files/TP-301-04.pdf

17. NHTSA. (1995, June 30). Laboratory Test Procedure TP-303-00. FMVSS 212 windshield mounting, FMVSS 219 windshield zone intrusion, FMVSS 303 fuel system integrity of compressed natural gas (CNG) vehicles. Washington, DC: Author. Available at www.nhtsa.gov/DOT/NHTSA/Vehicle%20Safety/Test%20Procedures/Associated%20Files/tp-303-00.pdf

18. NHTSA. (2006, December 15). Laboratory Test Procedure TP-214D-08 Side impact protection – Dynamic, standard regulation on dynamic side impact protection. Washington, DC: Author. Available at www.nhtsa.gov/DOT/NHTSA/Vehicle%20Safety/Test%20Procedures/Associated%20Files/TP214D-08Part1.pdf

(Appendixes A and B refer to the Side Impact Dummy. Appendix C, linked below, defines the aluminum honeycomb face on the moving barrier.)
www.nhtsa.gov/DOT/NHTSA/Vehicle%20Safety/Test%20Procedures/Associated%20Files/TP214D-08APP_C.pdf

19. NHTSA. (2007, January 17). Laboratory Test Procedure TP-301R-02 Fuel system integrity – Rear moving barrier impacts, standard regulation on fuel system integrity -- rear moving barrier impacts. Washington, DC: Author. Available at www.nhtsa.gov/DOT/NHTSA/Vehicle%20Safety/Test%20Procedures/Associated%20Files/TP-301R-02.pdf

20. NHTSA. (n.d.) Office of Vehicle Safety Compliance, compliance database. (Web site). Washington, DC: Author. Available at www.nhtsa.gov/cars/problems/comply/

21. Lemmon, E. W., Huber, M. L., & McLinden, M. O. (2013). NIST Standard Reference Database 23:  Reference Fluid Thermodynamic and Transport Properties-REFPROP, Version 9.1. Gaithersburg, MD: National Institute of Standards and Technology, Standard Reference Data Program. Available at www.nist.gov/srd/nist23.cfm

22. National Institute of Standards and Technology. (2011). Standard Reference Data, Thermophysical properties for helium. (Standard Reference Data, Web site). Gaithersburg, MD: Author. Available at http://webbook.nist.gov/chemistry/fluid/

23. NIST. (2008). Thermophysical Properties for Hydrogen.  (Standard Reference Data, Web site). Gaithersburg, MD: Author. Available at http://webbook.nist.gov/chemistry/fluid/

24. Post, M. B., Burgess, R., Rivkin, C., Buttner, W., O'Malley, K., & Ruiz. A. (2012, September) Onboard hydrogen/helium sensors in support of the global technical regulation: an assessment of performance in fuel cell electric vehicle crash tests. (Technical Report NREL/TP-5600-56177). Golden, CO: National Renewable Energy Laboratory. Available at www.nrel.gov/docs/fy12osti/56177.pdf

25. Society of Automotive Engineers.  (Revised July 2007) SAE J211: Instrumentation for impact test – part 1 – electronic instrumentation. Warrendale, PA: Author, Available  at http://standards.sae.org/j211/1_200707.

26. Society of Automotive Engineers. (Revised November 2009) SAE J2464: Electric and hybrid vehicle rechargeable energy storage system (RESS) safety and abuse testing – Recommended practices. Warrendale, PA: Author, Available  at http://standards.sae.org/j2464_200911

27. Society of Automotive Engineers.(Revised January 2009) SAE J2578 : Recommended practice for general fuel cell vehicle safety. Appendix A: Post-crash criteria for compressed hydrogen systems. Warrendale, PA: Author, Available  at http://www.sae.org/technical/standards/J2578_200901

28. Span, R., Lemmon, E. W.,  Jacobsen, R. T., Wagner, W., & Yokozeki, A. (2000). A Reference equation of state for the thermodynamic properties of nitrogen for temperatures from 63.151 to 1000 K and pressures to 2200 MPa Journal of Physical and Chemical Reference Data, Vol. 29, pp. 1361. Available  at http://link.aip.org/link/JPCRBU/v29/i6/p1361/s1.

29. Teleflex GFI, Control Systems Inc. 350 Bar Internal Solenoid Tank Valve Reference Manual TV-1XX Valves. GFIP224. (Issue 3: July 21, 2004).

30. UN 38.3 (E.09.VII.3) (2010) Lithium Metal and Lithium Ion Batteries. United Nations Economic Commission for Europe, Geneva, Switzerland. UN Manual of Tests and Criteria, Fifth Revised Edition. Part III Classification Procedures, Test Methods and Criteria Relating to Class 2, Class 3, Class 4, Division 5.1, Class 8 and Class 9, Section 38.3. Doc. Symbol ST/SG/AC.10/11/Rev.5; Sales No. E.09.VIII.3; ISBN 978-92-1-139135-0. Available at http://live.unece.org/fileadmin/DAM/trans/danger/publi/manual/Rev5/English/03en_part3.pdf

U.S. Department
of Transportation

**National Highway
Traffic Safety
Administration**

NHTSA

★★★★★

www.nhtsa.gov